3-D MULTICHANNEL SEISMIC REFLECTION STUDY OF VARIABLE-FLUX HYDROCARBON SEEPS, CONTINENTAL SLOPE, NORTHERN GULF OF MEXICO

A Thesis

by

RYAN DOUGLAS THOMAS

Submitted to the Office of Graduate Studies of
Texas A&M University
in partial fulfillment of the requirements of the degree of

MASTER OF SCIENCE

August 2003

Major Subject: Oceanography

3-D MULTICHANNEL SEISMIC REFLECTION STUDY OF VARIABLE-FLUX HYDROCARBON SEEPS, CONTINENTAL SLOPE, NORTHERN GULF OF MEXICO

A Thesis

by

RYAN DOUGLAS THOMAS

Submitted to the Office of Graduate Studies of
Texas A&M University
in partial fulfillment of the requirements of the degree of

MASTER OF SCIENCE

Approved as to style and content by:

William Sager (Chair of Committee)	William Bryant (Member)
Joel Watkins (Member)	Wilford Gardner (Head of Department)

August 2003

Major Subject: Oceanography

ABSTRACT

3D Multichannel Seismic Reflection Study of Variable-Flux Hydrocarbon Seeps, Continental Slope, Northern Gulf of Mexico. (August 2003)

Ryan Douglas Thomas,

B.S.; B.A., Michigan State University

Chair of Advisory Committee: Dr. William Sager

In the northern Gulf of Mexico, seafloor hydrocarbon fluid and gas seepage is an ubiquitous process on the continental margin. Although seafloor seepage and seep-related features (mud volcanoes, carbonate formation) have been studied for many years, little is known about their mechanisms of formation and the relationship of sub-surface structure to current seep activity. In this study, we examined three seafloor seeps in the Garden Banks and Mississippi Canyon areas using exploration and reprocessed 3D multi-channel seismic (MCS) data augmented with side-scan sonar (Garden Banks site) to characterize hydrocarbon seep activity and develop an understanding of the processes that led to their formation. Side-scan sonar data provided high resolution coverage of the seafloor while the exploration seismic data were used to image near and deep sub-surface features. Additionally, the 3D amplitude extraction maps were useful in delineating amplitude anomalies often associated with seep related activity. The reprocessed 3D seismic data were used to map in greater detail near seafloor features and amplitude anomalies.

Using remote sensing geophysical data, we were effectively able to map sub-surface features such as salt topography, seep-related faults and geophysical indicators of hydrocarbons and correlate them with seafloor amplitude anomalies and fault traces in order to characterize seep activity level. The southern mud volcano in the Garden Banks site is characterized as an established high flux seep vent owing to signs of active seepage and sediment flows as well as the build-up of hard grounds. The northern mud volcano in the area, with greater hard ground build-up and fewer signs of active seepage represents an established low flux seep vent. In the Mississippi Canyon area, the data suggest that the seep mound can be characterized as a mature high flux vent due to the extensive build-up of hard ground, evidence of gas hydrates and signs of active seepage and sediment flows.

The mechanisms of formation are similar between the two study sites. Upwelling salt appears to have fractured the sub-surface leading to the formation of fault induced depressions. Mapping of geophysical indicators of hydrocarbons implies that hydrocarbon migration is occurring along bedding planes to the fault systems underlying the depressions. Here they appear to migrate vertically to the seafloor creating the topographic features and seafloor amplitude anomalies that characterize the seeps.

ACKNOWLEDGMENTS

I would like to thank Dr. William Sager, chairman of my advisory committee, for acquiring the multichannel seismic data and providing support and guidance throughout my time at Texas A&M University. Additionally, I would like to thank Dr. William Bryant and Dr. Joel Watkins for their knowledge and advice as committee members and Sandy Drews in the Department of Oceanography for her guidance and making sure I filled out all the proper paperwork. I am pleased to have met so many pleasant and knowledgeable individuals at Texas A&M University.

I would also like to thank Western Geco, Inc. for the data and reprocessing as well as DOE NETL for providing the funding for 3D MCS reprocessing. Finally, I would like to extend my appreciation to Texas A&M University and the Department of Oceanography for allowing me to attend and complete my Master's degree.

TABLE OF CONTENTS

LIST OF TABLES

LIST OF FIGURES

FIGURE Page

CHAPTER I

INTRODUCTION

Seafloor venting of hydrocarbon fluid and gas is a naturally occurring phenomenon on the continental margin in the northern Gulf of Mexico (Anderson and Bryant, 1987; Reilly et al., 1996). If over-pressured fluids and gas deposits exist at depth in the sub-surface, they may migrate vertically and laterally through the sediment column along fault planes, sedimentary bedding planes, or through permeable stratigraphic units to create "seep mounds" or "mud volcanoes" on the seafloor (Hovland and Judd, 1988; Roberts, 1995; Kaluza and Doyle, 1996; Dimitrov, 2002; Orange et al., 2002; Sager et al., 2003). These seep mounds and their associated features are of interest because they occur in areas that may contain substantial accumulations of gas hydrate, a methane ice-like substance that is both a trophic source for chemosynthetic communities and a potential alternative energy source (Kvenvolden, 1993; Sassen et al., 1998). Additionally, every offshore petroleum field development site in the Gulf must be evaluated for potential geohazards as pressurized fluid and gas deposits as well as seep features pose a threat to offshore structure installations (Corthay, 1998; Roberts et al., 1999). Evaluation and identification typically occurs through geophysical means (e.g. seismic, side-scan sonar) as geophysical data are able to show us a great deal about the structure and geology of a seep, which may enhance our understanding of seep processes and the environmental conditions that favor their formation.

This thesis follows the style and format of the Bulletin of the American Association of Petroleum Geologists

In this study, I attempt to characterize hydrocarbon seep activity and develop an understanding of the processes that lead to seep formation. Two areas observed to contain prolific seeps, Garden Banks lease blocks 424-425 and Mississippi Canyon lease blocks 852-853 (Figure 1) were surveyed using 3D exploration multi-channel seismic (MCS) (McDonald et al., 2000; Sassen et al, 1999b). In this case, a high resolution MCS volume was reprocessed from the original exploration data to enhance the resolution of each data set. Hydrocarbon fluid and gas seeps often exhibit well-known acoustic anomalies in the geophysical record such as seafloor reflection amplitude anomalies, zones of chaotic and attenuated reflectors as well as bright spots that may be associated with gas charged sediment, active venting and hard ground formation (Roberts, 1992; Roberts et al., 1996; Corthay, 1998; Riedel et al., 2002; Sager et al., 2003). Indeed, the feasibility of using MCS data to interpret and characterize seafloor seeps and their associated anomalies has been established by previously published studies and site investigations (Trabant, 1996; Roberts et al., 1996; 1999; 2002; Riedel et al., 2002; Sager et al; 2003).

Geologic Setting

The slope of Texas and Louisiana is about 180 to 240 km wide covering an area from the continental shelf break south to the Sigsbee Escarpment with water depths ranging from 200 meters to 3400 meters below sea level (Bryant et al., 1990). The uneven topography of the northern Gulf of Mexico is attributed to the mobilization of underlying Jurassic salt by sediment loading during times of low sea-stand (Bryant et al.,

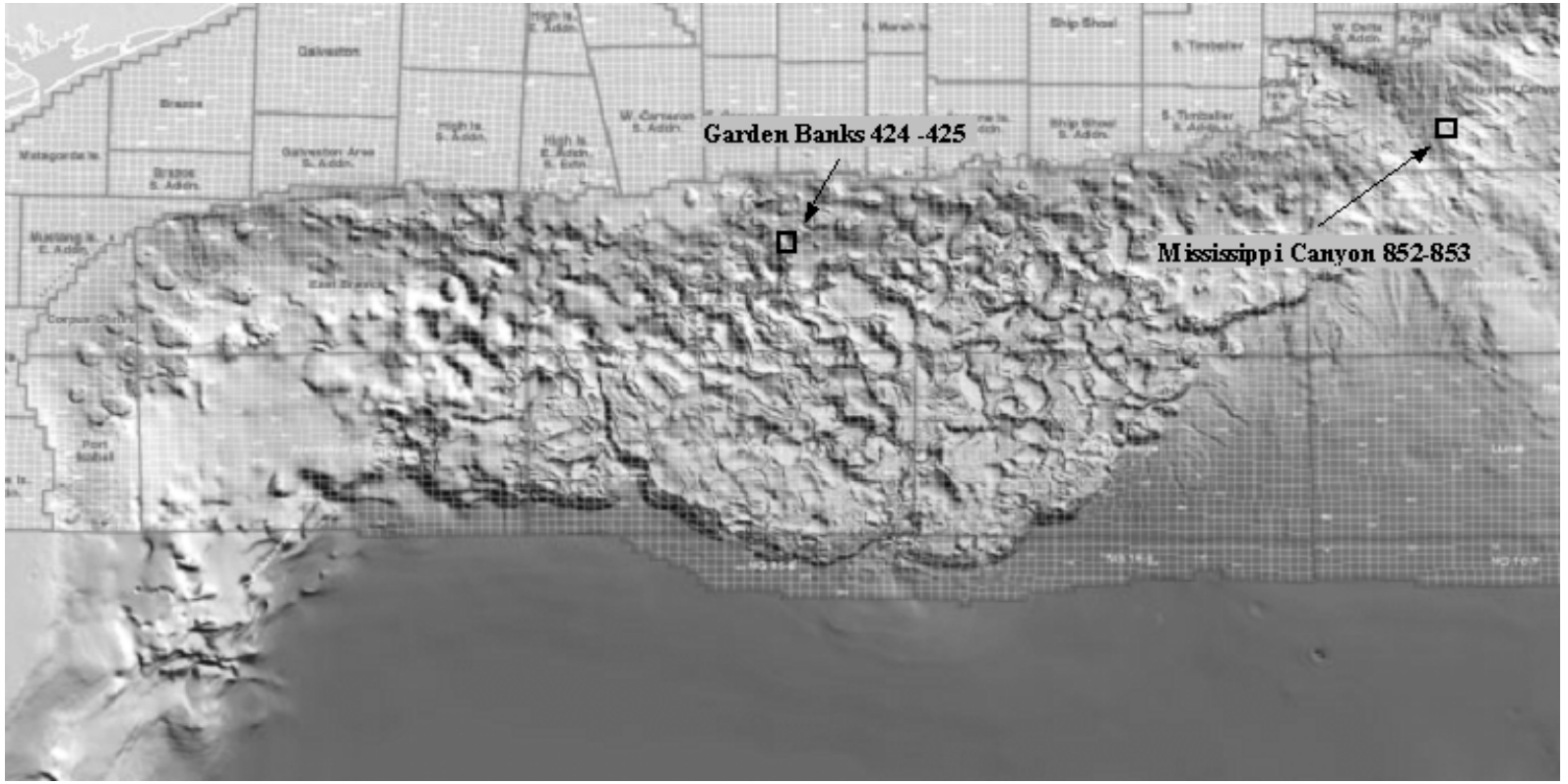

Figure 1. Bathymetric map of the northern Gulf of Mexico indicating the two study areas, Garden Banks 424-425 and Mississippi Canyon 852-853. *Image used with permission by Dr. William Bryant and The Deep Tow Group, Texas A&M University.*

1990; Schuster, 1995). The weight of the overlying sediments causes the salt to extrude upwards or laterally in search of equilibrium, taking on a variety of morphologies, primarily salt diapirs on the shelf and upper slope and salt sheets on the middle and lower slope (Schuster, 1995; Rowan, 1995). This halokinesis of allochthonous salt has led to the formation of the dome and basin morphologies that are found across the Gulf of Mexico's northern slope (Schuster, 1995). The domes represent the presence of salt in the shallow sub-surface, visible on sub-bottom and seismic records, whereas the basin and graben structures typically represent the withdrawal of salt from the area or flanking by surrounding salt diapirs (Bryant et al., 1990; Roberts et al., 1990; 1996). Frequently the salt motion fractures the overlying sediment with regional growth faults and other more complex fault systems (Kaluza and Doyle, 1996; Rowan et al., 1999). When these systems intersect with sub-surface reservoirs, pressurized hydrocarbons and gas may migrate along the faults from deep reservoirs to the seafloor leading to the wide spectrum of hydrocarbon seeps (volcanoes, carbonate mounds, craters) and related features (fluidized mud flows) that have been identified across the Gulf of Mexico's northern slope (Anderson and Bryant, 1987; Neurauter and Bryant, 1990; Roberts and Carney, 1997).

Garden Banks (GB) lease blocks 424-425 contain several seep features overlying a complex fault system on the southwestern flank of a large salt dome. The two most prominent seeps, identified as active mud volcanoes, have been the focus of several prior studies involving high-resolution side-scan sonar and sub-bottom profiler systems to characterize surficial and near-surface features (Lee, 1995; Sager et al., 1999; 2003;

MacDonald et al., 2000; Mullins, 2001). Submersible dives and piston core studies have been conducted to catalogue seep related features and more recently, exploration 3D MCS studies to map out regional structure and fault systems (Lee, 1995; Sager et al., 1999; 2003).

The second area of focus, Mississippi Canyon (MC) lease blocks 852-853, is located on the western flank of the Mississippi Canyon atop a structural high over a relatively shallow (3.5 sec two-way travel time) salt body. This site contains a large hydrocarbon fluid and gas seep mound that is located near the edge of a salt withdrawal basin and is thought to be the release site for fluid and gas migrating laterally along bedding planes out of the Ursa field petroleum basin located within and to the north of the survey area (Sassen, 1999b). Coring studies in the area indicate that gas hydrate deposits are present and observations from submersible dives on the seep mound note the occurrence of carbonate outcrops and bacterial mats as well as active seepage (Sassen, 1999b; Milkov and Sassen, 2000).

Classification of Seep Morphological Features

A generalized relationship appears to exist between the flux rate of a seep and the vent-seep features that develop (Roberts and Carney, 1997). Flux rates tend to be divided into three categories: (1) Low flux rates characterized by extensive authigenic carbonate formation and a lack of vent sites as well as mud flows, (2) transitional flux rates, which may lead to gas hydrate or carbonate formation as well as fluid and gas expulsion features and (3) high flux rates, which tends to lead to the formation of mud

volcanoes characterized by active vent sites and sediment flows (Roberts and Carney, 1997; Sager et al., 2003). Seeps exhibiting low to transitional flux rates may contain authigenic carbonates which are formed by the precipitation of calcium carbonate as a byproduct of microbial oxidation of hydrocarbons (Roberts et al., 1990; 1997). They tend to occur in thin layers or as mound features in the shallow sub-surface or on the seafloor (Roberts et al., 1990).

Gas hydrates, which may form at seeps characterized by transitional flux rates are compounds composed of natural gas locked in a crystalline lattice of water molecules. They form on or within slope sediments where high pressure and low temperature favor their formation from hydrocarbon gas (Milkov and Sassen, 2000; Lowrie, 2002). Hydrate mounds are considered to be mud volcanoes that contain gas hydrate, but in some cases the mounds themselves can be composed entirely of hydrate itself (Neurauter and Bryant, 1990; MacDonald et al., 1994; Kaluza and Doyle, 1996). They are assumed to be abundant on the Gulf's northern continental slope because of the large amount of hydrocarbon gases that vent to the seafloor from the sub-surface (Sassen et al., 2002). Unlike other continental margins, where gas hydrates are predominately of biogenic origin and occur at a depth of several hundred meters, the Gulf of Mexico's massive fault systems allow thermogenic gasses and other fluids to rise rapidly to the seafloor resulting in the creation of hydrate bodies at or near the seafloor (MacDonald et al., 1994; 2000).

A third geological feature normally associated with high flux rates is the mud volcano, a generic term that also refers to mud mounds, mud ridges or mud diapirs,

depending on their mechanism of formation (Dimitrov, 2002). Whatever the morphology, formation is typically dependent on over-pressured fluids, gases and unconsolidated sediment migrating along fault planes to the seafloor, resulting in cone shaped accumulations of mud (Neurauter, 1988; Roberts, 1995). Mud mounds occur throughout the world's oceans and continental lowlands, wherever sub-surface, over-pressurized sediments find a conduit to the seafloor. They are especially prevalent on the Gulf of Mexico's continental slope and typical mounds can range from a few meters to over one kilometer in diameter with up to 150 meters of relief (Roberts, 1995; Kaluza and Doyle, 1996; Sager et al., 1998). Many large mud mounds exhibit a rounded, irregular or flat-topped summit with a central caldera from which liquid mud may vent from the sub-surface (Roberts, 1995; Kaluza and Doyle, 1996). Although their mechanism of formation is not well known, it is generally assumed that flat and round-topped mounds occur through sedimentary volcanism, while irregular topped mounds may be related to mud diapirism (Kaluza and Doyle, 1996; Sager et al., 2003).

It is thought that seep mounds go through a three stage self-sealing process culminating with a carbonate crust or mound forming over the main migration pathway (Hovland, 2002). The first stage is the development of bacterial mats in the near to shallow sub-surface. The second stage occurs when sediment becomes trapped in the migration pathways with the bacterial mats growing to exposure at the seafloor. Finally, it is thought that the reduced flow or vertical flux allows carbonate to build up and block migration pathways, effectively sealing or capping the seep (Kaluza and Doyle, 1996; Hovland, 2002).

Active seeps do not always create vertical relief features, but almost all affect topography in some way or another. Negative relief and no-relief seep-related features affect the topography in the form of pockmarks, craters, and fluidized-mud flows (Hovland and Judd, 1988; Roberts et al., 1990; Kaluza and Doyle, 1996). According to Hovland and Judd (1988), pockmarks can be defined as the erosion or removal of sediment from the seafloor, usually in association with fluid or gas expulsion. Pockmarks exhibit a variety of shapes, mostly elliptical, circular, or asymmetrical and generally occur in the vicinity of salt domes and fault systems. Sizes range from a few meters to hundreds of meters in diameter with a few meters negative relief (Hovland and Judd, 1988; Kaluza and Doyle, 1996). Large fluid expulsion features are commonly referred to as seafloor craters, which can be the result of over-pressured gas surging to the seafloor. Large, explosive releases of gas can lead to craters hundreds of meters in diameter and hundreds of meters deep which may expel debris and fluid visible at the sea surface (Kaluza and Doyle, 1996).

Another common seep related feature found on the northern slope are fluid vents from which flows of brine or watery sediment may originate. Generally seen in side-scan sonar records as an area of high acoustic backscatter, flows can occur in association with other features such as mud and hydrate mounds or originate from a fault on the seafloor. Flows can be composed of viscous, brecciated sediment, which do not travel far, or low-viscosity fluidized mud, which may travel many kilometers before settling (Linimov et al., 1997). While verification of a seep location can be conducted with sediment coring or by direct observation with submersibles or ROV, it is a seep's

acoustic response or geophysical signature during high-resolution site surveys that leads to initial identification and classification.

Geophysical Signatures of Fluid and Gas Seeps

Although geophysical signatures of hydrocarbon fluid and gas seeps vary, common characteristics have been defined. In seismic sections it is generally found that (1) seeps have an amorphous appearance in contrast with the surrounding stratified sediment, (2) the amorphous appearance gradually expands with depth until merging with regional chaotic sequences, (3) shallow sediment layers are up-turned along the seeps lateral boundaries, (4) most major seeps are linked to prominent faults and (5) large quantities of free gas are commonly present in and around the active seep locations (Neurauter and Bryant,1990; Roberts et al., 1990; 1999)

There is a wide range of geophysical responses to hydrocarbon deposits including acoustic wipeout, bright spots, acoustic turbidity, velocity pull-downs and multiples (Table 1). The most widely occurring anomaly is acoustic wipeout, in which the seismic signal may be attenuated or absorbed by free gas in the sub-surface allowing little or no energy to be reflected (Roberts, 1992; Sager et al., 2003). Frequently, this response is associated with mound structures and seeps, but can also occur where large concentrations of gas are present in the sub-surface, such as in ancient river channels and estuarine environments (Anderson and Bryant, 1990). Wipeout may also be caused by near total reflection of acoustic energy off a hard-bottom or other surface with a large

Table 1. Acoustic anomalies associated with hydrocarbon fluid and gas deposits. Data compiled from Hovland and Judd, 1988; Behrens, 1988; Anderson and Bryant, 1990; Sager et al., 2003.

Feature	Characteristic	Description
Acoustic Wipeout (Simple Wipeout)	Absence of sub-surface reflectors	Attenuation of signal by sub-surface free gas or Near total reflection of signal due to large acoustic impedance mismatch, such as hard bottom or other dense material.
Ringing (Reverberant Wipeout)	Prolonged acoustic echo above an acoustic void	Reverberation of acoustic signal caused by gas bubbles, carbonate, biogenic debris or other seep related material. Creates multiple reflections of the same reflector in the data record underlain by an acoustic void.
Bright Spots	Enhanced sub-surface reflectors	Localized amplitude enhancement of sub-surface reflectors while preserving primary reflectors. Caused by acoustic amplitude mismatch such as boundary between water saturated and gas/hydrocarbon-saturated sediments. Phase reversal of signal indicates that gas or hydrocarbons are present.
Amorphous Return (Acoustic Turbidity)	Chaotic sub-surface reflectors	Scattering of the acoustic signal in the upper sediment column due to the presence of free gas or debris. Signal is reflected but reflectors are chaotic or cloudy in the sub-bottom and seismic profile record.
Multiples	Multiple reflections of the same primary reflector	Large acoustic impedance at or beneath the seafloor (carbonate hard ground, gassy sediment) reflects the acoustic signal where it is then re-reflected at the sea surface. The pattern repeats, sometimes masking real primary reflectors, until the acoustic signal dissipates.
Bottom Simulating Reflector (BSR)	Sub-surface reflector cross-cutting other sediment reflectors	Free gas trapped below a gas hydrate layer leads to a reflection due to the large impedance mismatch. Because of hydrate stability requirements the boundary, and hence the reflection, mimics the seafloor, cross-cutting other sub-surface reflectors. May be confused with multiples.
Velocity Pull-down	Apparent downward dipping or warping of horizontal reflectors	Results from a reduction of seismic sound speed at the edge of a large gas body or gas chimney. Sound travels slower through gaseous sediments, therefore increasing travel time as it return to the source/receiver.

acoustic impedance contrast, in which little energy penetrates the boundary. Water saturated sediments, when juxtaposed to gas saturated sediments, will sometimes lead to large acoustic impedance contrasts that produce localized amplitude enhancements or "bright spots" in the data which preserves horizons in the data but increases their amplitude. Although other causes of impedance contrasts can lead to amplitude enhancement, a phase reversal at the bright spot is a strong indicator that free gas is responsible (Anderson and Bryant, 1990).

Amorphous return or "acoustic turbidity", as it is sometimes termed, generally occurs when sound is scattered by gas or debris in the upper sediment column, resulting in a cloudy or chaotic appearance (Hovland and Judd, 1988; Anderson and Bryant, 1990). Another anomalous feature is velocity pull-down, in which the reflectors apparently dip downwards at the edge of a large gas body or gas chimney due to a reduction in sound velocity (Anderson and Bryant, 1990). Finally, if a large acoustic-impedance contrast is present at the seafloor or the sub-surface, be it carbonate hard ground, high gas concentrations or other seep related material, some of the acoustic energy could be reflected and then re-reflected at the sea surface with this pattern repeating itself until the acoustic signal energy has dissipated (Behrens, 1988; Sheriff and Geldart, 1995). These reflections can mask real primary reflections on sub-bottom and seismic profile records and are generally referred to as "multiples". Though not detected in the study areas presented in this paper, other anomalies may result in relation to gas and hydrocarbon seeps, such as bottom simulating reflectors and "ringing".

It is important to note that the acoustic frequency of the acquisition system, hydrocarbon deposit characteristics as well as the presence of carbonates and other hard-bottoms plays a major role in the type of anomaly or anomalies that may occur in the data record. Acoustic wipeout, multiples, acoustic turbidity, bright spots and others are all dependant on the amount of gas, fluid and seep debris present in the sediment column as well as the density, distribution and the size of individual gas bubbles (Anderson and Bryant, 1990; Sheriff and Geldart, 1995).

When 3D MCS data are available, seeps can be found to produce reflection amplitude anomalies at the seafloor (Roberts et al., 1996; Mullins, 2001; Sager et al., 2003). Identifying anomalies involves mapping out the seafloor horizon in a 3D seismic data set, then displaying the seismic wave amplitude at the horizon in map view for interpretation. Amplitude anomalies at the seafloor are caused by changes in the reflection coefficient of the seafloor and shallow horizons. For example, positive amplitude anomalies most likely indicate an increase in seismic velocity, such as one would expect from a carbonate crust, gas hydrate or other dense material accumulation (Roberts et al., 1996, Reilly et al., 1996, Sager et al., 2003). In prior studies, seismic amplitude attribute maps were used in conjunction with visual observations and coring to successfully locate and verify the presence of hard-bottoms in areas of positive amplitude anomalies, and gassy sediments in areas of low amplitude anomalies (Roberts et al., 1996; Reilly et al., 1996). Dense data coverage and the ability of 3D seismic data to delineate gas charged sediments and areas of hard ground makes amplitude attribute maps a valuable reconnaissance and interpretative tool. As more data correlating

seafloor features and their associated seismic response are collected and analyzed, we may be able to distinguish between different seep-related features based on the waveform of their seismic amplitude response alone (Roberts et al., 2002).

Side-scan sonar is also an effective geophysical tool when imaging seeps in that it has the ability to show differences in the properties of surficial sediments. Sonars construct a seafloor image by sending out an acoustic pulse and displaying the amplitude of the sound returned from the seafloor backscatter. Backscatter is a function of surface roughness and sediment grain size (Fish and Carr, 1990). Therefore, at seep locations sonar data can delineate fluidized mudflows that have disturbed seafloor sediments, fault traces and fluid expulsion features (Kaluza and Doyle, 1996; Roberts and Doyle, 1998, Sager et al., 1998; 2003; Dimitrov, 2002). Having somewhat similar response mechanisms, sonar features can be compared with those found in amplitude maps, the differences leading to a better understanding of seep surface characteristics.

CHAPTER II

DATA AND METHODS

The primary data used in this study were exploration and reprocessed 3D MCS data collected and reprocessed by Western Geco, Inc. The original exploration data were processed at a 4 msec sampling rate and then interpolated to a common depth point (CDP) inline spacing of 12.5 x 25 m for the Garden Banks volume and 13.5 x 26.5 m for the Mississippi Canyon volume. Frequency analysis determined the frequency range to be 6-128 kHz after filter application. The short-offset 3D MCS volume was reprocessed from the original data tapes at a sampling rate of 2 msec and a high band pass filter was applied to produce a frequency range of 20 to 128 kHz. Near incident traces were utilized in the reprocessed data to produce 9 fold stacks, as opposed to the 30 (GB) and 51 (MC) fold stacks created in the original 3D MCS exploration data. Additional acquisition parameters of the 3D MCS data are given in Table 2.

The Garden Banks site was also surveyed with 12 kHz side scan sonar. Image swaths 3000 m in width were collected along north - south oriented ship tracks spaced 1500 meters apart, resulting in 200% sonar coverage of the area (Sager et al., 1998). Sonar data were collected using differential GPS satellite navigation with accuracy of better than 5 meters. An acoustic tracking system was used to determine layback of the fish, which was situated approximately 240 meters behind and 50 meters below the vessel (Sager et al., 1998).

Table 2. Acquisition and reprocessing parameters of 3D MCS data
GB = Garden Banks, MC = Mississippi Canyon

Description		**Original 3D MCS**	**Reprocessed 3D MCS**
Type of Source		Dual Airguns	Unchanged
Recorded Sampling Interval		2 ms	Unchanged
Processed Sampling Intereval		4 ms	2 ms
Filter	Lo Cut	6 Hz	20 Hz
	Hi Cut	128 Hz	128 Hz
Shot Point Interval MC		40.0 meters	Unchanged
Receiver Interval MC		26.6 meters	Unchanged
Shot Point Interval GB		53.3 meters	Unchanged
Receiver Interval GB		25.0 meters	Unchanged
Nominal Fold MC		30	9
3D Bin Size MC		53.3 x 13.3 meters	Unchanged
Nominal Fold GB		51	9
3D Bin Size GB		40.0 x 12.5 meters	Unchanged

The original and reprocessed 3D seismic volumes were examined using a seismic interpretive program, Kingdom Suite v. 6.2. Seafloor time contour maps were created by manually interpreting every 5th in-line and cross-line at each study site. Due to the large impedance contrast of the sediment-water interface creating a strong coherent reflector, the program was allowed to autopick infill lines across the seafloor of the study areas. The resultant infill lines were then inspected for erroneous time (z) values and checked with time values from proximal lines. Time data were converted to depth using a sound velocity of 1500 m/sec. Due to the pervasive deformation and distortion of the geophysical record by the presence of gas and hydrocarbons in the sub-surface, a full structural analysis was not attempted. Fault interpretation was done on cross section profiles as well as time slices and then compared with side scan sonar images, when available, to produce a final interpretation.

CHAPTER III

RESULTS

Garden Banks Lease Blocks 424-425

Bathymetry extracted from reprocessed 3D MCS data reveals the Garden Banks site as being dominated by two north-south oriented active vent features, a southern mud volcano (SMV) and a northern mud volcano (NMV) (Figure 2). At a depth of 580 meters, the SMV has a diameter of about 1.7 km and exhibits relief up to 80 meters above the surrounding seafloor. The summit appears flat topped with a small area of positive relief (20 m) on the eastern side of the summit. On the other hand, the NMV has a diameter of about 1.25 km with local relief up to 40 meters. The NMV's summit is uniformly flat with no apparent relief. West of the volcanoes lies a shallow flat-floored depression trending north-south across the survey area with water depths ranging from 640 to 670 meters. Located directly east of the mounds is a southwestern dipping slope that extends past the 800 m isobath at the SE edge of the survey boundary. An east-west trending salt-induced ridge characterizes the northern boundary of the study site with localized relief ranging from 10 to 100 meters and a maximum side-slope of about 12°. The south end of the survey site contains a westward dipping fault scarp separating the shallow depression to the west and the slope to the east. The scarp is readily visible from the southern edge of the survey area northward to the southeastern flank of the SMV.

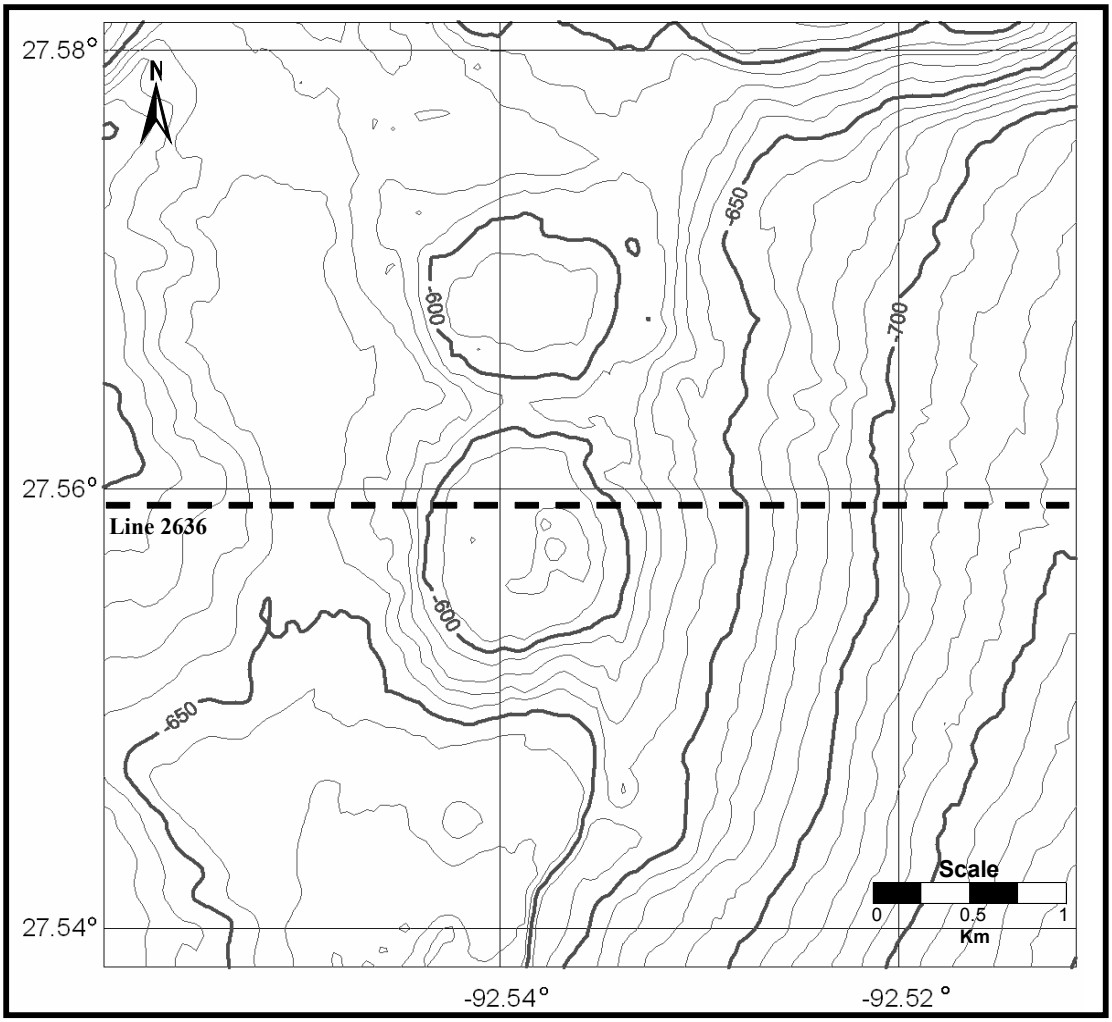

Figure 2. Bathymetric map of the Garden Banks lease blocks 424-425 study site. Bathymetric data were extracted from reprocessed 3D MCS data set for this area. Contours at 10-meter intervals, calculated from two-way travel time using 1500 m/s. Heavy dashed line shows profile in Figure 8.

Side-Scan Sonar Data

The SMV was observed to be active by Sager and others (1999) and MacDonald and others (2000). Sonar data shows the summit as an area of high backscatter except for two patches on the east and southwestern edges where low backscatter or dead spots are observed (Figure 3). The flanks of the SMV appear to exhibit low to medium backscatter on all but the northern flank where two linear fault traces extend to the southern edge of the NMV.

The NMV's summit also exhibits high backscatter, suggesting that it is capped with carbonate or other coarse debris. There exist small areas of low backscatter at the center and southwest edge of the summit, similar to the SMV's east-side patch, which may indicate the presence of gas charged sediment or active venting since gas absorbs the acoustic pulse, resulting in low backscatter. The flanks of the NMV return a higher backscatter than the SMV's. The NMV has not been the focus of any major studies; therefore coring or observational data is not available.

Southeast of the two mud volcanoes, a north-south trending fault trace is discernable on the sonar record (GS/FT in Fig. 3). Sediment disturbances associated with this fault appear as linear high backscatter features. As the fault approaches the volcanoes, additional linear traces from discrete faults intersect with the main fault as it trends north. East of the volcanoes another high backscatter feature, thought to be a fluidized sediment flow (SF in Fig. 3), appears to emanate from between the mud volcanoes and trends eastward down the slope out of the survey area. Other high backscatter sediment flows appearing to originate from the western flank of the SMV

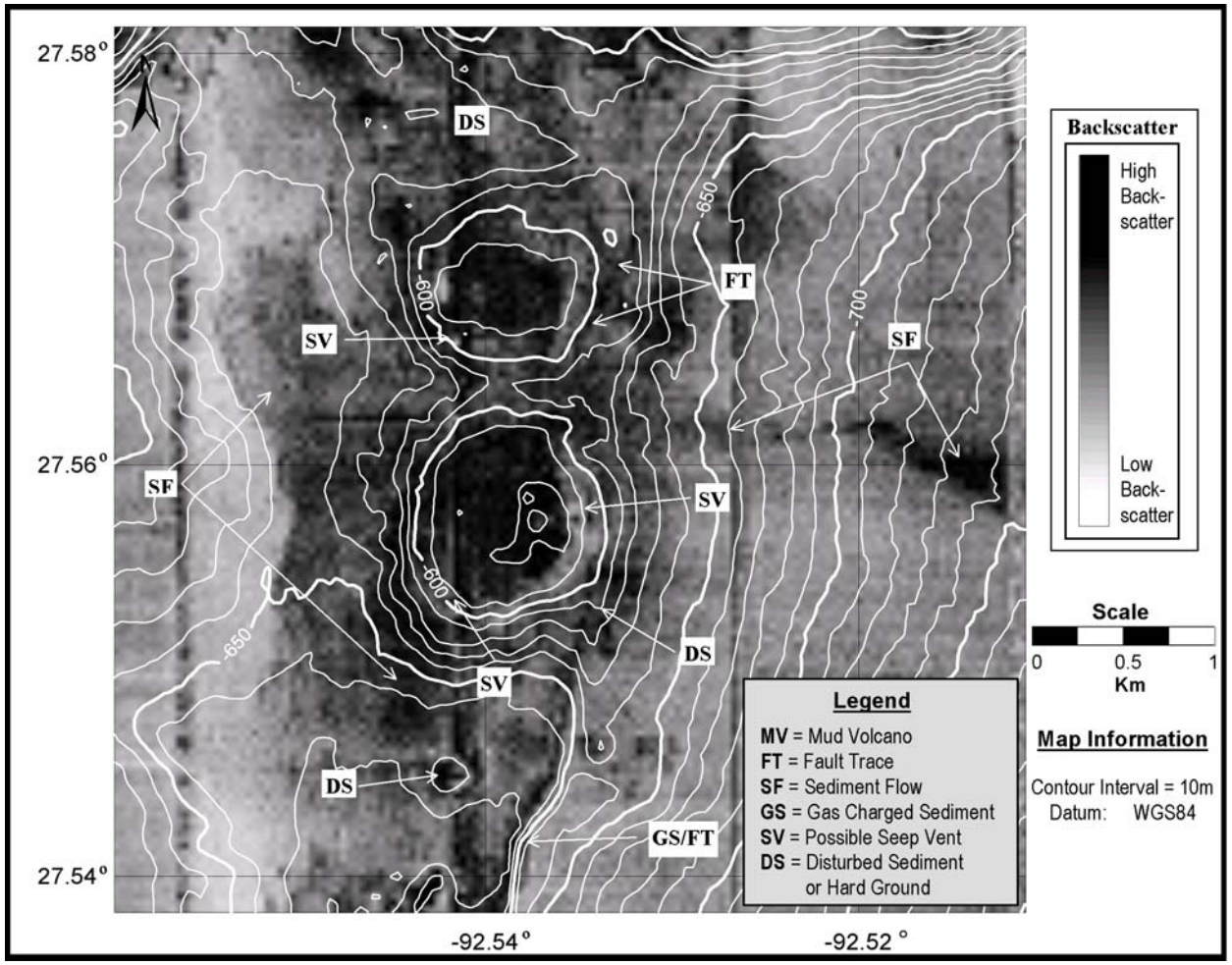

Figure 3. Side-scan sonar image overlaid with bathymetric contours of the Garden Banks site. Dark areas represent high acoustic backscatter whereas lighter areas show low backscatter. Labels describe seep related features (see text).

superimpose the shallow depression west of the volcanoes (SF in Fig. 3). Finally, large areas of high backscatter are present at the north end of the survey area most likely due to seep related changes to the sediment as well as the coalescing of faults in this area.

3D MCS Amplitude Data

The amplitude response of the SMV summit is largely neutral to negative in comparison with the area's overall response (Figures 4 and 5). Patches of positive amplitude anomalies (higher velocities) are evident on the southern edge of the summit in both the original and reprocessed 3D MCS images. In contrast, on the northwestern edge, the reprocessed MCS data also displays a positive amplitude response. This discrepancy is possibly related to differences in the vertical resolution between the two data sets (see discussion). Negative amplitude anomalies (lower velocities) are present on the eastern and western flanks, corresponding for the most part with areas of low backscatter in the sonar image.

The amplitude response of the NMV's summit appears more positive than that of the SMV. On the southwest edge, a strong negative amplitude response 80 m in diameter, usually associated with gas charged sediment or venting, appears in both the original and reprocessed 3D MCS data sets. Inconsistencies are apparent between the two data sets when viewing the amplitude response from the NMV's flanks. Both data sets return positive amplitude anomalies on the southern and western flanks, but the reprocessed data characterizes the northern and eastern flanks as more positive than the

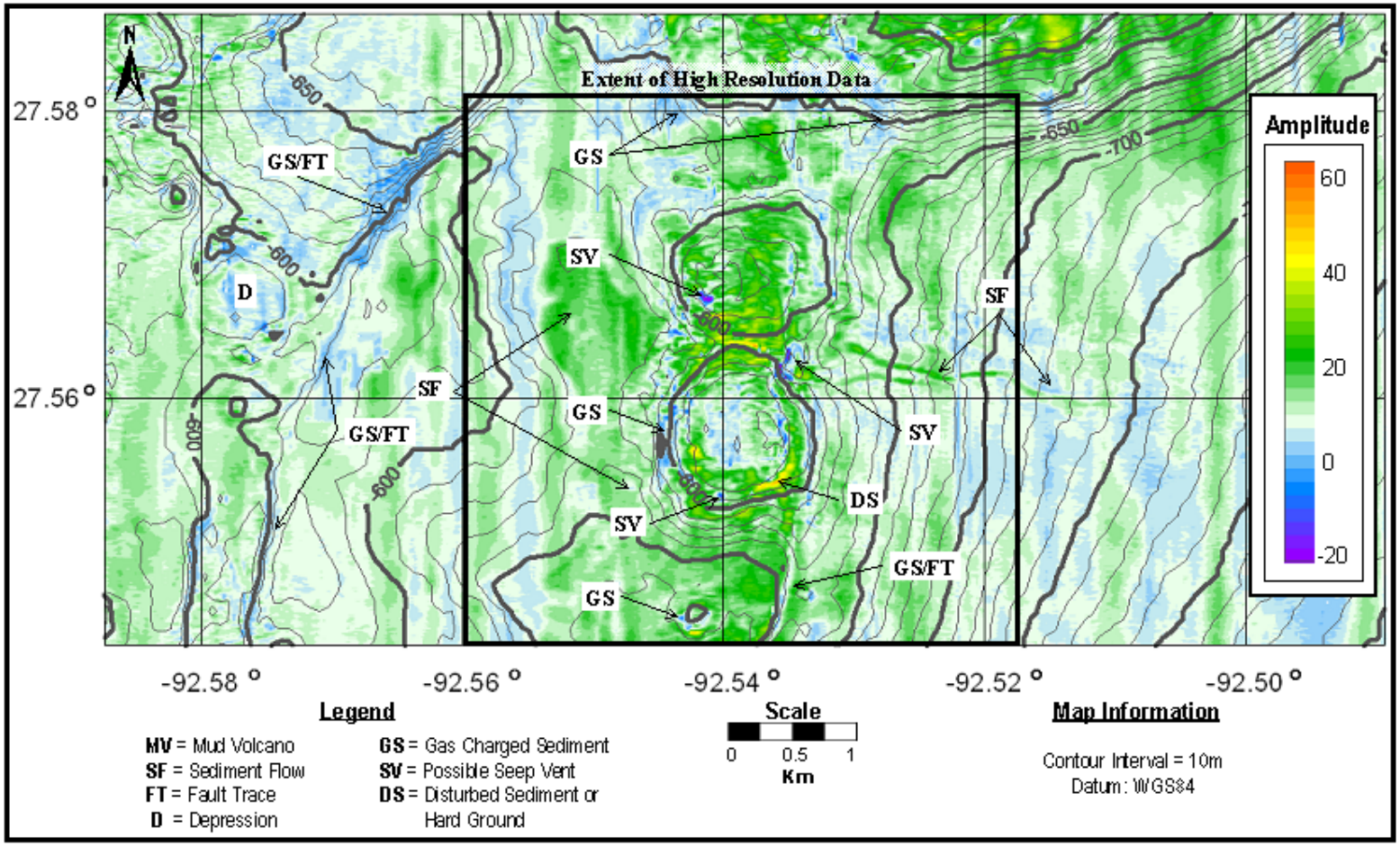

Figure 4. Exploration 3D MCS seafloor amplitude map of the Garden Banks site. Bathymetric contours were extracted from exploration 3D MCS data set for this area. Labels describe seep related features. Warm colors denote positive amplitudes, whereas cool colors show negative. Amplitude scale in arbitrary units.

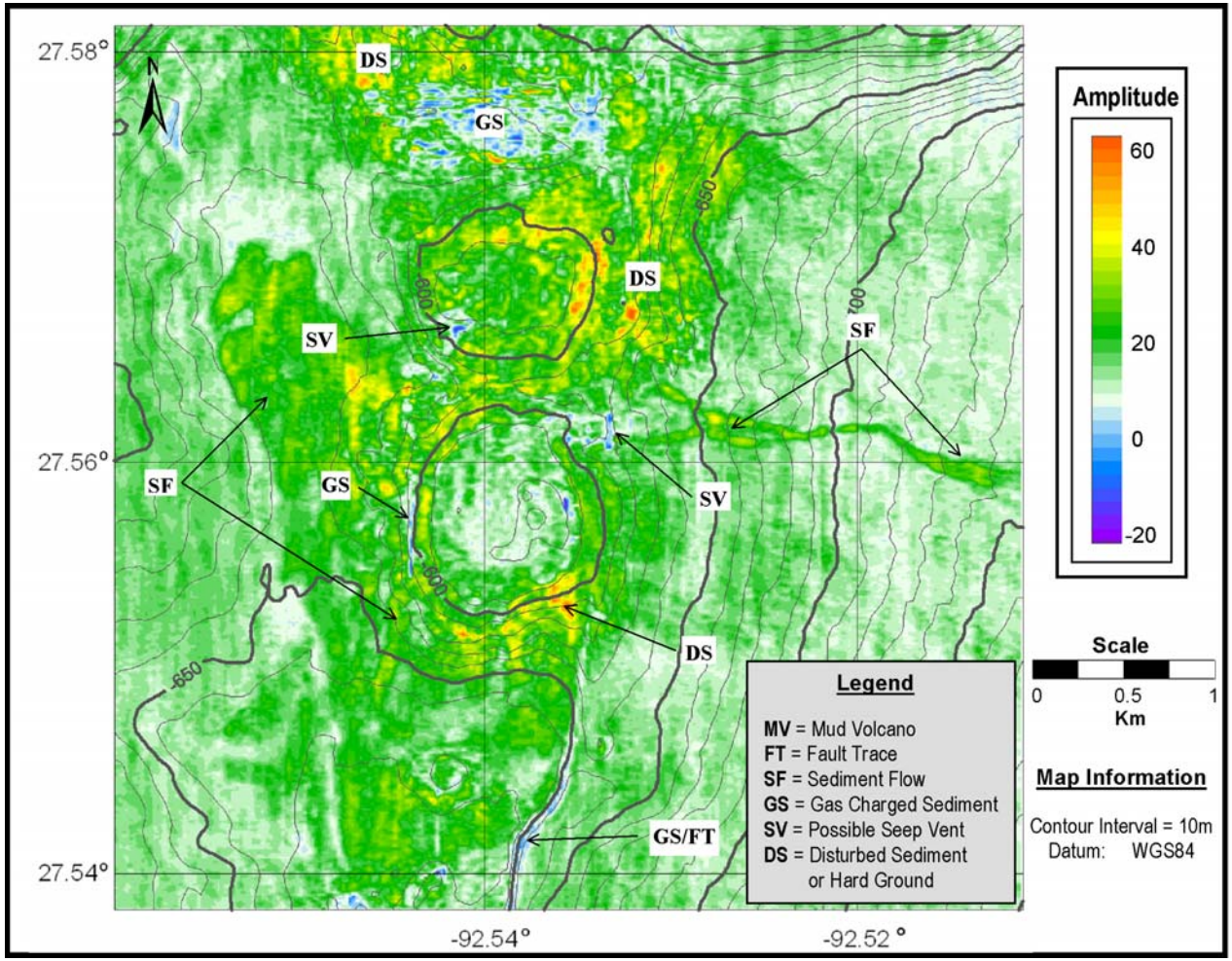

Figure 5. Reprocessed 3D MCS seafloor amplitude map of the Garden Banks site. Bathymetric contours were extracted from reprocessed 3D MCS data set for this area. Labels describe seep related features. Color scale same as Figure 4.

original data, with the original MCS data even showing patches of negative amplitudes on the eastern flank.

South of the central mud volcanoes, a linear fault-related negative amplitude anomaly is present, correlating with the linear high backscatter feature at –92.539° longitude in the side-scan sonar record (GS/FT in Fig. 3). Other positive and negative amplitude anomalies located east of the mud volcanoes may also be related to this fault as it continues north through the area.

The amplitude map suggests the presence of two sediment flows in the area. The first is the eastward trending flow appearing to originate from the negative amplitude anomaly, most likely related to the main fault on the east side of the mud volcanoes (SF in Figs. 4 and 5). The second is a broad flow that has collected in the topographic low to the west of the mud volcanoes, which appears to emanate from the west-southwest flank of the SMV (SF in Figs. 4 and 5). Both correspond to the interpreted sediment flows in the side-scan sonar record.

3D MCS Reflection Data

The topography and structure of the Garden Banks site appears to be mainly influenced by the salt ridge it overlies (Figure 6). Salt is shallowest at the north end of the survey where it peaks at 1.8 sec TWT. The two mud volcanoes are located atop the north-south trending ridge that extends south from the northern salt ridge. The salt drops off sharply to the east past the bottom of the data at 6.0 sec TWT and to the west forming a shallow depression that underlies the topographic depression on the west side

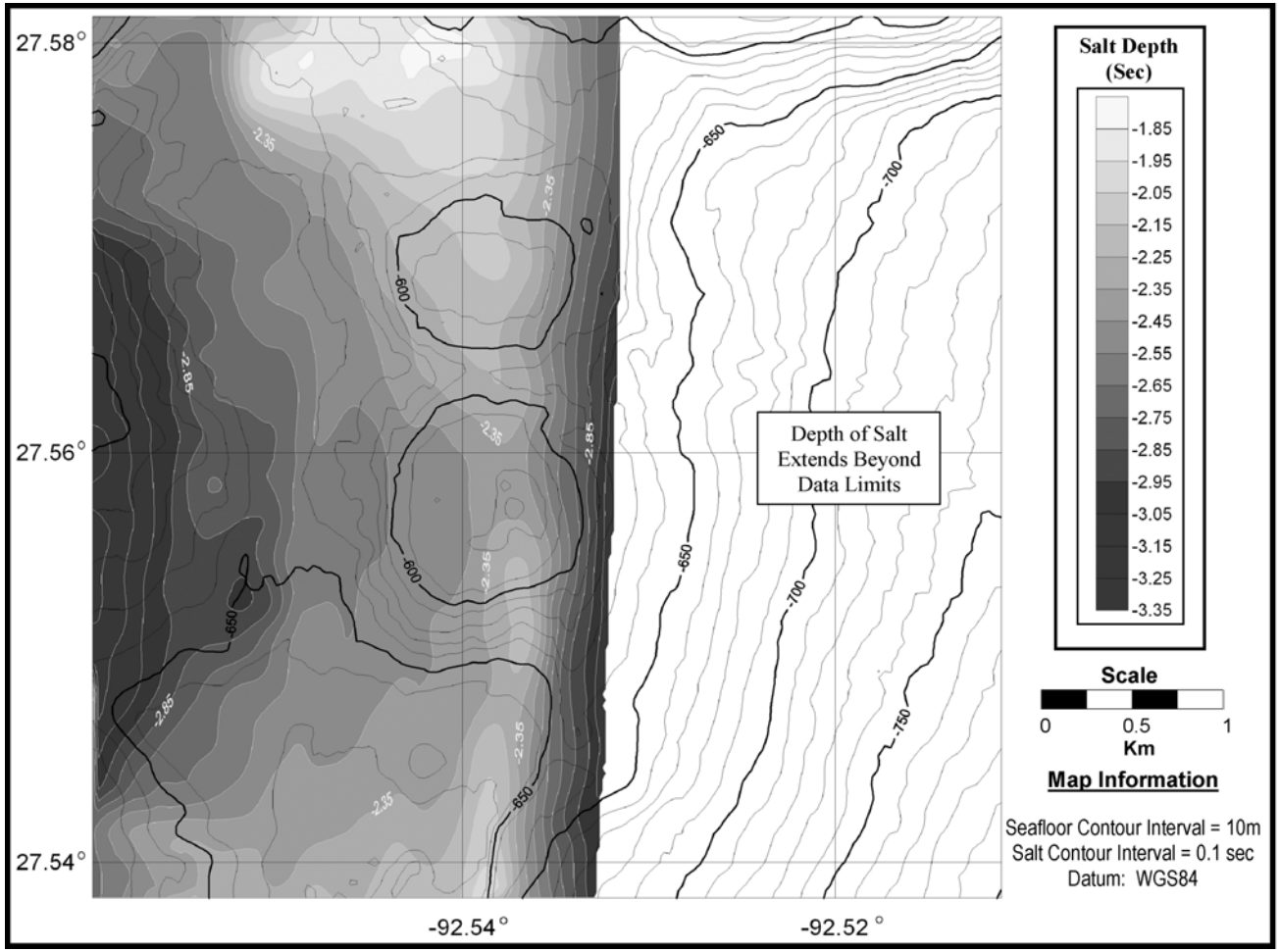

Figure 6. Top-of-salt topography in relation to seafloor topography in the Garden Banks site. Black contours represent seafloor topography whereas the shaded contours represent salt topography. The eastern boundary of the salt appears linear due to cut-off of driving salt ridge flank.

of the survey area. Underneath the slope on the east side of the survey area, the salt dips sharply eastward past the vertical extent of the data set at 6.0 sec TWT.

Above the salt, the sub-surface can be characterized as chaotic. Pervasive deformation, diffractions from fractured bedding planes and geophysical indicators of gas have affected the clarity of the sub-surface reflections. Strong reflectors, possibly caused by the existence of hard grounds and coarse debris on and around the mud volcanoes, have led to the presence of multiples at 1.6 sec TWT to 1.8 sec TWT masking low amplitude reflectors in the sub-surface (Figure 7). The multiple is oriented north to south and has an east to west extent of about 2-4 km.

The regional dip of sub-surface reflectors is generally eastward with localized increases in dip occurring beneath the mud volcanoes (Figure 8). Evidence of a widespread unconformity exists in the area with multiple reflectors terminating at this feature in both the original and reprocessed data sets. The unconformity is disrupted by a large synthetic fault with an offset of 0.5 sec TWT originating from near the apex of the underlying salt ridge and trending north south. This fault corresponds to the fault trace visible on the seafloor in the side-scan sonar and 3D MCS amplitude maps to the south and east of the mud volcanoes. As the fault continues north, multiple discrete faults form at the southern extent of the SMV and accompany the main fault to the survey area's northern boundary (Figure 9). In response to the synthetic fault, counter regional faults have formed to the west of the mud volcanoes and extend to 1.7 sec TWT where they appear to truncate at the synthetic fault. No major seep related faults have been detected to the east of the mud volcanoes except for multiple localized fractures

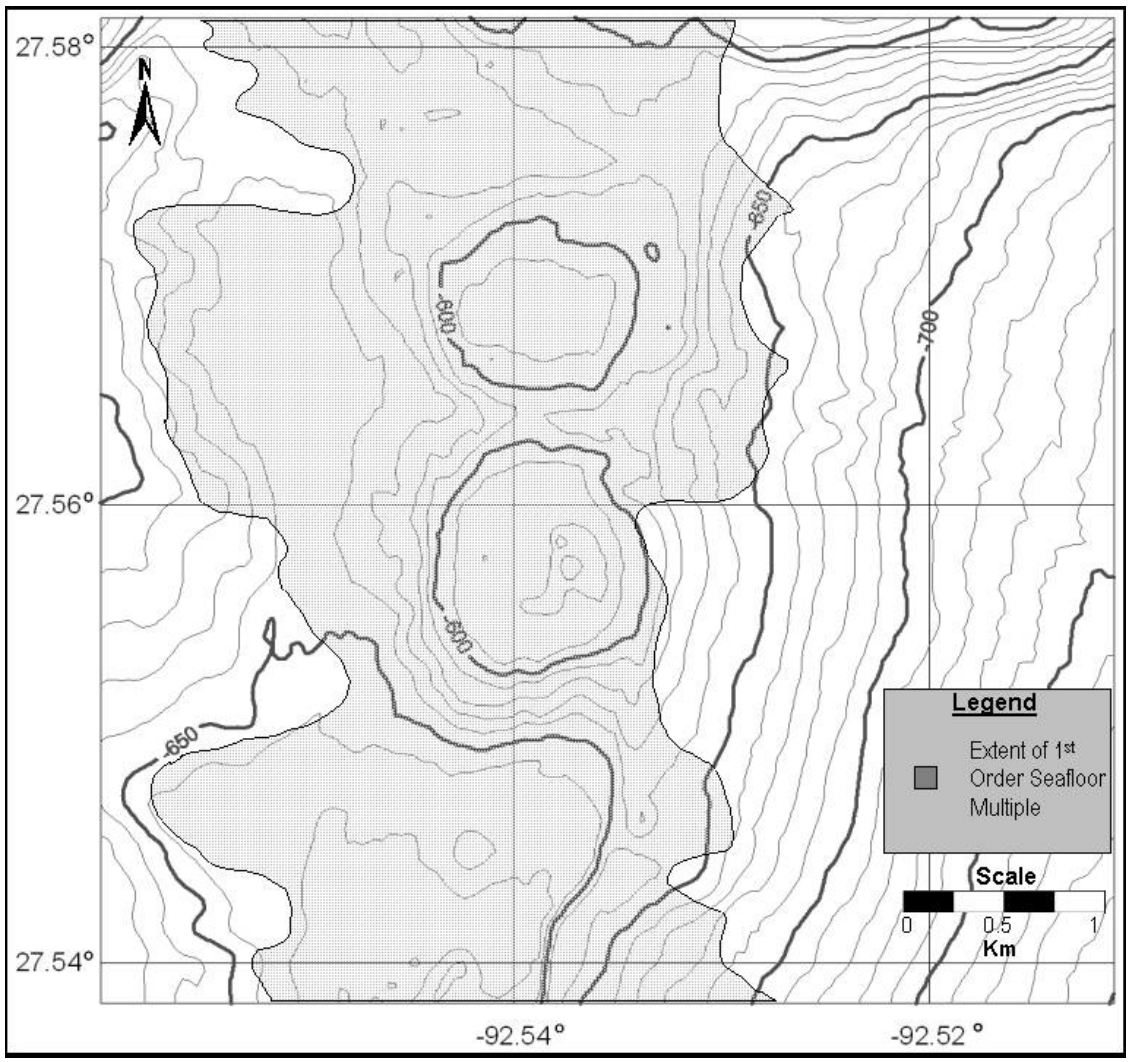

Figure 7. Bathymetric map illustrating lateral extent of 1st order seafloor multiple in the original and reprocessed 3D MCS data in the Garden Banks site.

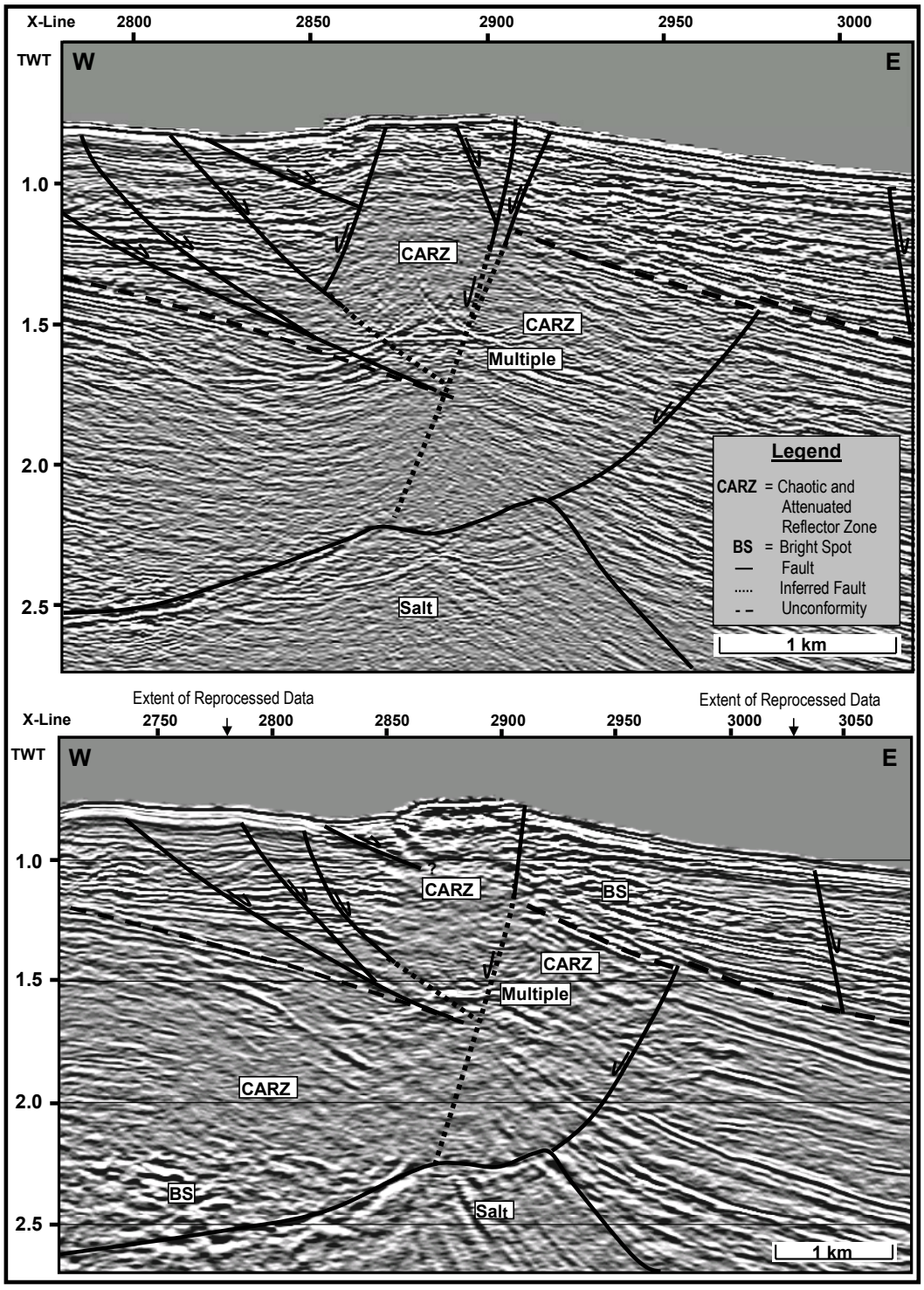

Figure 8. Cross-section of reprocessed (top) and original (bottom) 3D MCS data across west to east profile line 2636 in the Garden Banks site. Location in Figure 2.

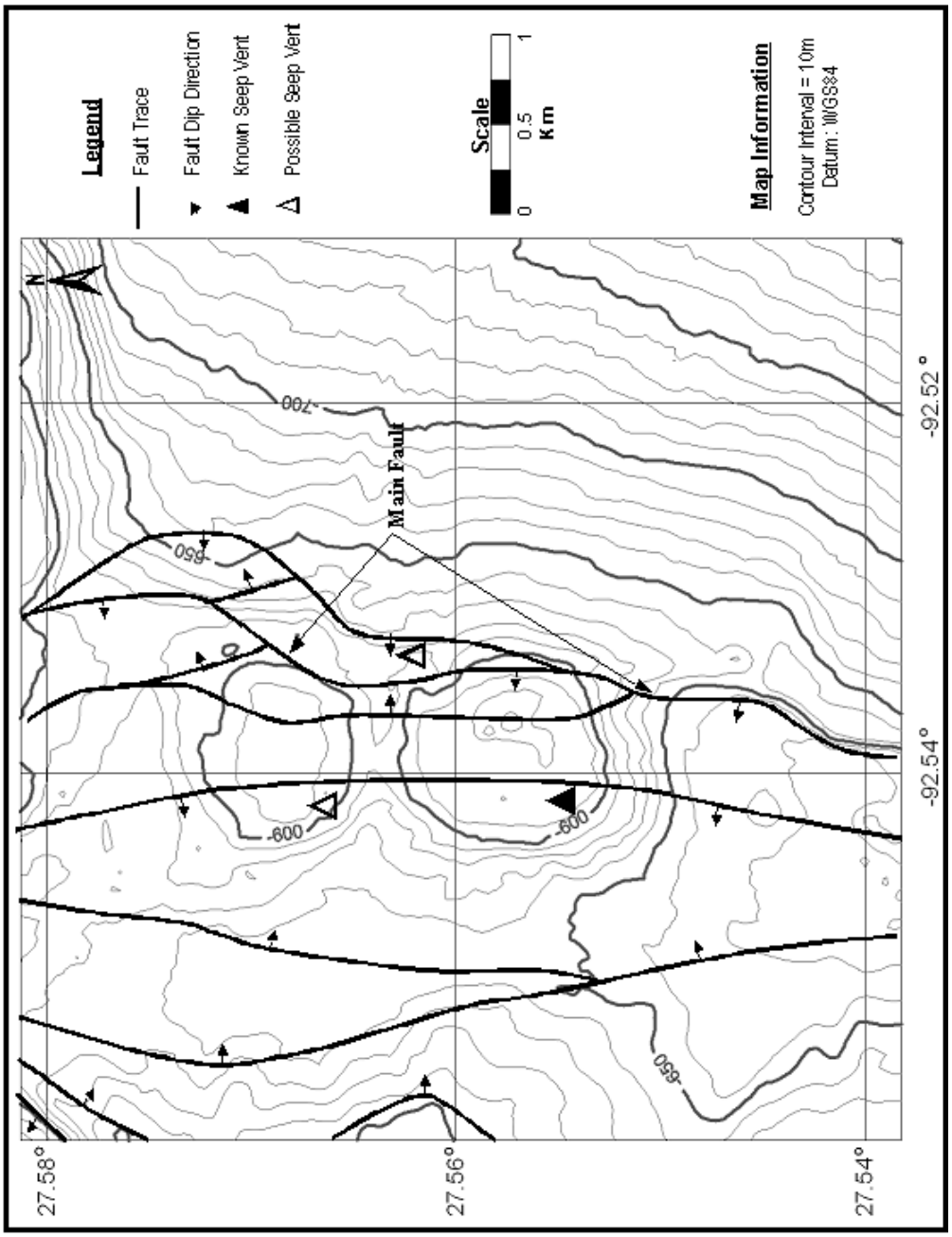

Figure 9. Map illustrating location of seep related faults as well as known and assumed vent locations in the Garden Banks area.

and a westward dipping normal fault extending from the apex of the salt ridge between shot points 2900-2950 to 1.4 sec TWT in the sub-surface.

Geophysical indicators of possible hydrocarbon fluid and gas deposits including attenuated and chaotic reflectors as well as bright spots are present in the area. The mapping of these indictors in cross-sections as well as time slices shows the probable hydrocarbons located within 0.75 sec TWT of the sediment-salt interface from the western and northwestern boundaries of the survey area to the north-south oriented salt ridge crest beneath the mud volcanoes (Figure 8). Here the gas appears to travel vertically through the faulted sub-surface creating a zone of chaotic and attenuated reflectors that extends up to the summits of the mud volcanoes and is possibly related to gas migration or poor imaging due to presence of hard grounds. Zones of chaotic reflectors and bright spots also occur in the eastern portion of the survey area around 1.5 sec TWT at shot points 2900 - 2950 to a point west of the small fault extending from the salt ridge crest. In the south, disrupted reflectors are present beneath the fault scarp of the main synthetic fault as well as beneath a small fluid or gas expulsion feature 500 m west of the fault scarp.

Mississippi Canyon Lease Blocks 852 – 853

Bathymetry (Figure 10) extracted from the original 3D MCS data volume reveals the seafloor as sloping from west to east at an average of 2°. Breaking the slope in the center of the survey area is a 1.0 x 1.5 km mound at the 1000 m isobath exhibiting about 40 m of relief. The summit shows signs of variable relief with topographic highs

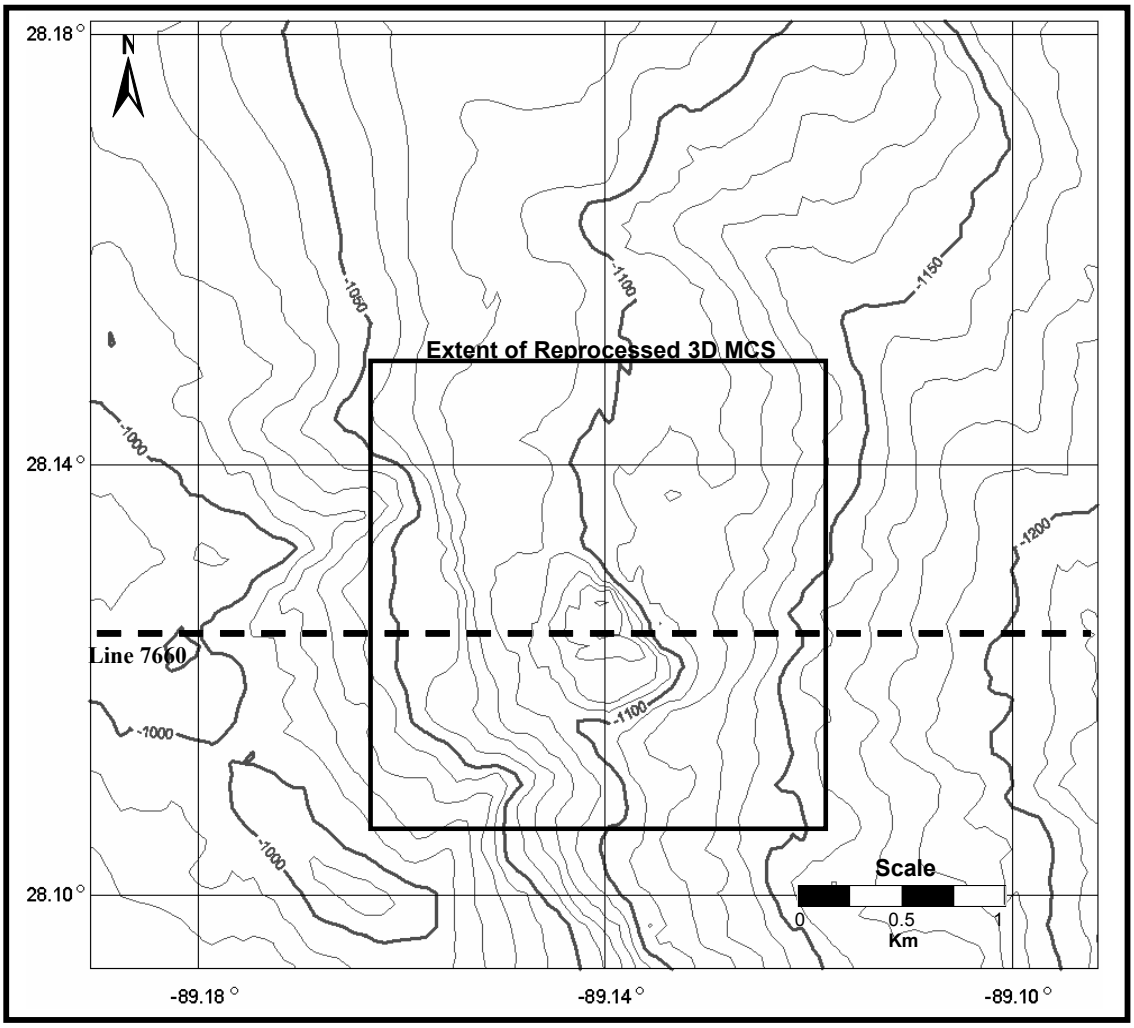

Figure 10. Bathymetric map of the Mississippi Canyon lease blocks 852-853 study site. Bathymetric data were extracted from exploration 3D MCS data set for this area. Conventions as in Figure 2

appearing on the eastern edge and lows occurring around the center. The mound is located about 1 km east of a broad southeast trending ridge bounded on the east by a 20 m relief fault scarp. The northern and eastern portions of the survey area are characterized as mostly horizontal seafloor incised with eastward trending channel-like features exhibiting one to ten meters of negative relief possibly caused by the down slope movement of sediments.

3D MCS Amplitude Data

Relative to the survey area's average amplitude response the summit of the mound is characterized by positive amplitude anomalies on the northern and southern edges and negative anomalies at its center and eastern edge (Figures 11 and 12). The positive anomalies generally correspond with the mounds topographic highs except for the small pinnacle on the eastern summit which returns neutral to negative amplitudes. The largest collection of negative anomalies corresponds with the topographic low at the center of the mound's summit. Both the original and reprocessed data sets display a negative amplitude band on the eastern flank of the mound, but the original data also displays negative anomalies on the southeastern and western flanks as well.

The amplitude maps suggest the presence of two sediment flows in the area, a broad area of positive amplitude response directly east of the mound and another occupying a shallow depression to the west-northwest of the mounds flank (SF in Figs. 11 and 12). The fault scarp at the base of the ridge appears as a negative amplitude anomaly (GS/FT in Figs. 11 and 12). The western portion of the survey area is

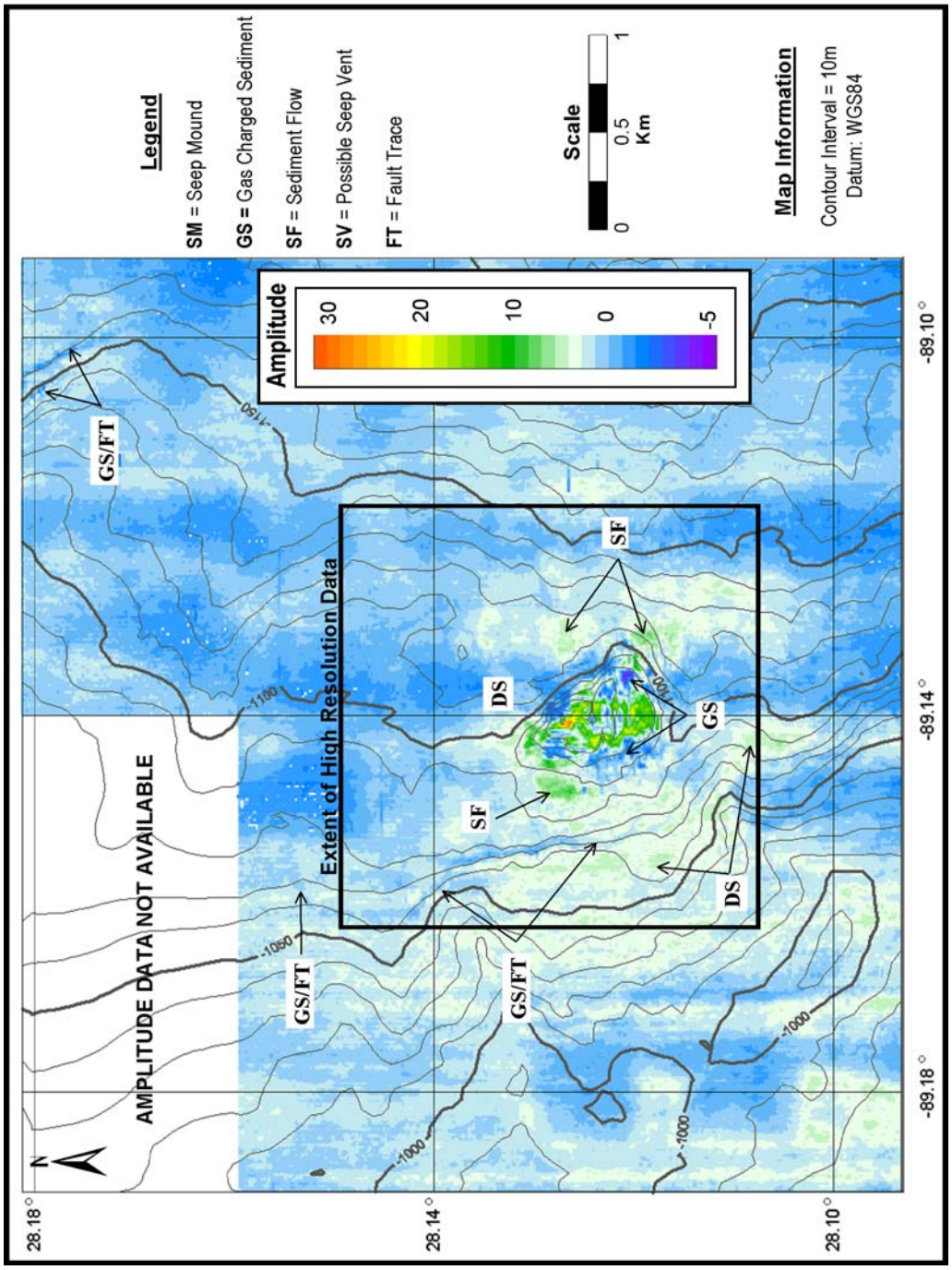

Figure 11. Seafloor amplitude map of the Mississippi Canyon site from exploration 3D MCS data. Conventions as in Figure 4. Note: Color scale units different than in previous amplitude figures.

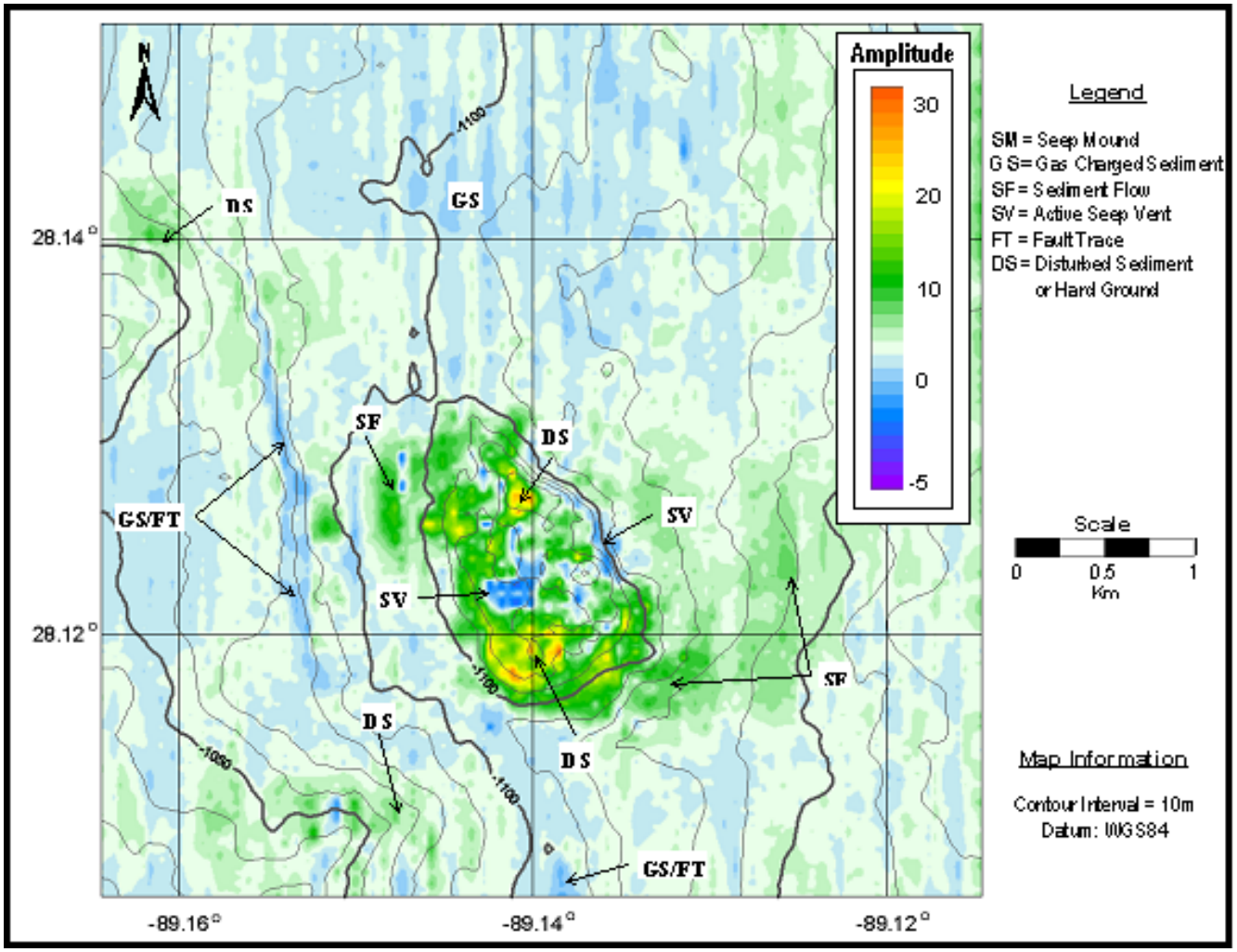

Figure 12. Seafloor amplitude map of Mississippi Canyon site from reprocessed 3D MCS data. Conventions as in Figure 5.

characterized by neutral amplitude responses except for patches of positive anomalies that appear to overlie two eastward oriented ridges, one 1.5 km southwest and the other 2 km northwest of the central mound feature (DS in Figs. 11 and 12). The rest of the survey area contains few amplitude anomalies except for two fault-related northwest-southeast trending negative anomalies at the northeastern boundary (GS/FT in Figs. 11 and 12) and small patches of negative amplitudes that may be fault-related to the north and northeast of the mound. Throughout the area, the north-south oriented narrow bands of negative amplitude responses that appear are most likely artifacts of seafloor horizon interpretation.

3D MCS Reflection Data

The underlying body of salt exhibits topographic highs in two locations within the Mississippi Canyon study area (Figure 13). The first occurs 400 meters southeast of the central mound structure where the salt forms a north-south oriented ridge, which crests at 2.5 sec TWT. The second occurs in the northeast corner of the survey area where the salt crests at 2.8 sec TWT. East of the central ridge, the salt dips sharply east past the bottom of the 3D MCS data. The remaining salt body underlying the study area maintains an average depth of 4 sec TWT except for two topographic lows, one a 1.8 km diameter shallow depression 2 km to the west of the mound and the other a NW-SE trending 1 km wide depression separating the central and northeastern salt crests.

As in the Garden Banks MCS, the seismic reflectors in the Mississippi Canyon site show evidence of pervasive deformation throughout with chaotic and hummocky

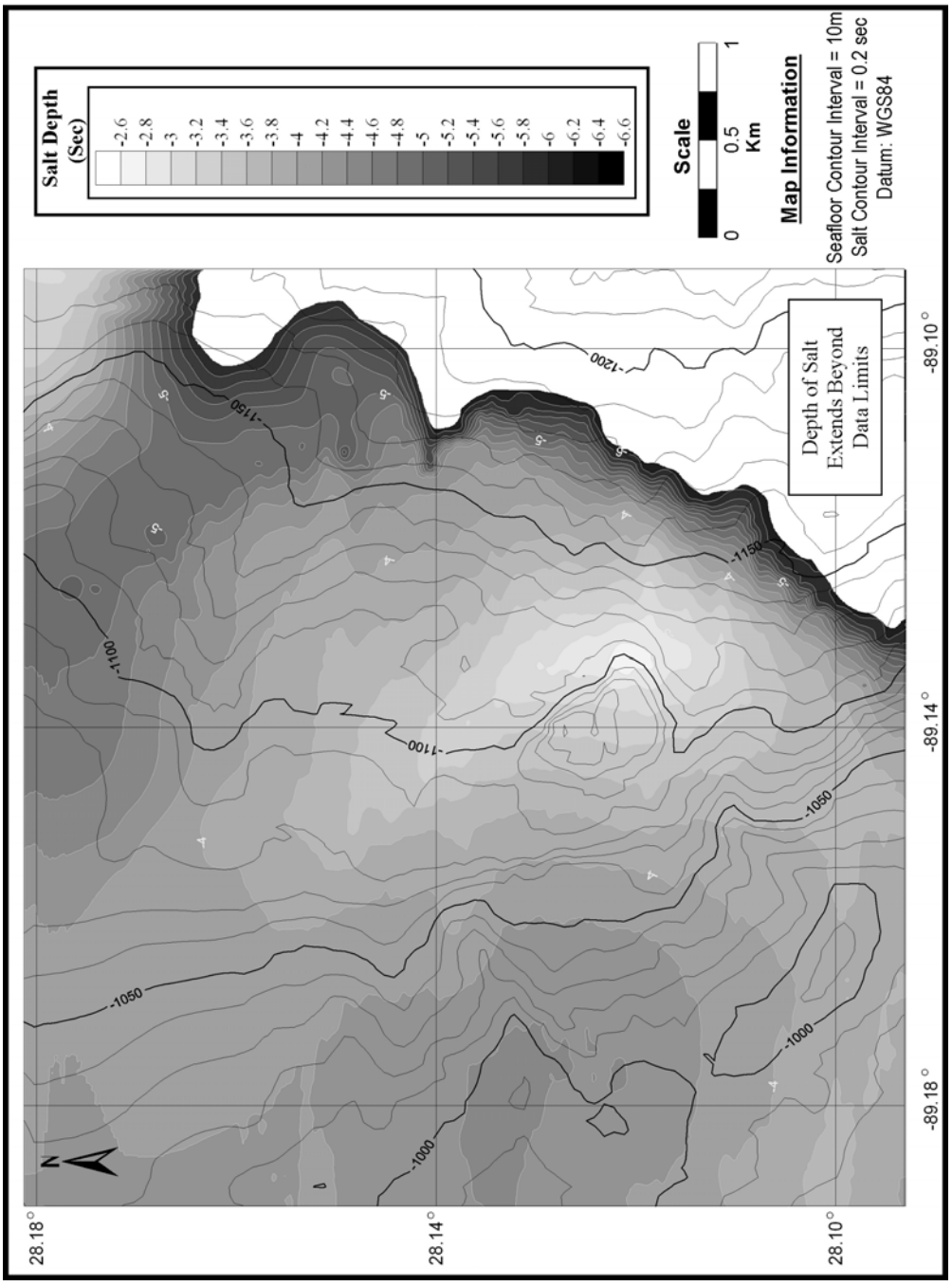

Figure 13. Salt topography in relation to seafloor topography in the Mississippi Canyon site. Contours represent seafloor topography whereas the shaded contours represent salt topography.

styles characterizing the reflectors in areas where geophysical indicators of hydrocarbon fluid and gas are present and beneath the hard grounds on the mound's summit. A low amplitude multiple is present at 2.9 sec TWT in both the original and reprocessed 3D MCS data. The seafloor multiple was traced to the northern and southern extent of the reprocessed MCS survey data and appears to extend no wider than 2 km east to west (Figure 14). Sub-surface horizons remain fairly horizontal in the upper 2 sec TWT but tend to mimic the salt topography as depth increases (Figure 15). Reflectors below 2 sec TWT appear tilted as they approach the topographic highs and lows of the underlying salt, with the most steeply dipping reflectors occurring to the immediate east and west of the central salt ridge around 2.5 to 3.5 sec TWT.

A series of elliptical shaped normal faults encompass the central mound feature (Figure 16). The largest, outermost of these faults appears to extend to the salt interface between 2.8 and 3.2 sec TWT, correlating with the fault scarp in the bathymetric and 3D MCS seafloor amplitude map. Small antithetic faults have formed at the flanks and central portion of the mound truncating into the surrounding synthetic faults at a depth of around 2.0 sec TWT. In the eastern portion of the survey area, large north-south trending synthetic and antithetic faults have formed over the steeply dipping salt in that area extending to 3.0 sec TWT (Figure 15). In the west, shallow dipping faults (no deeper than 1.6 sec TWT) between shot points 4800 and 4850 may be responsible for the formation of the valley and ridge morphology that characterizes the western face of the SE trending ridge. Additionally, 1 km to the east and 1.5 km to the west of the central mound, small normal faults are found to encompass fluid or gas expulsion features

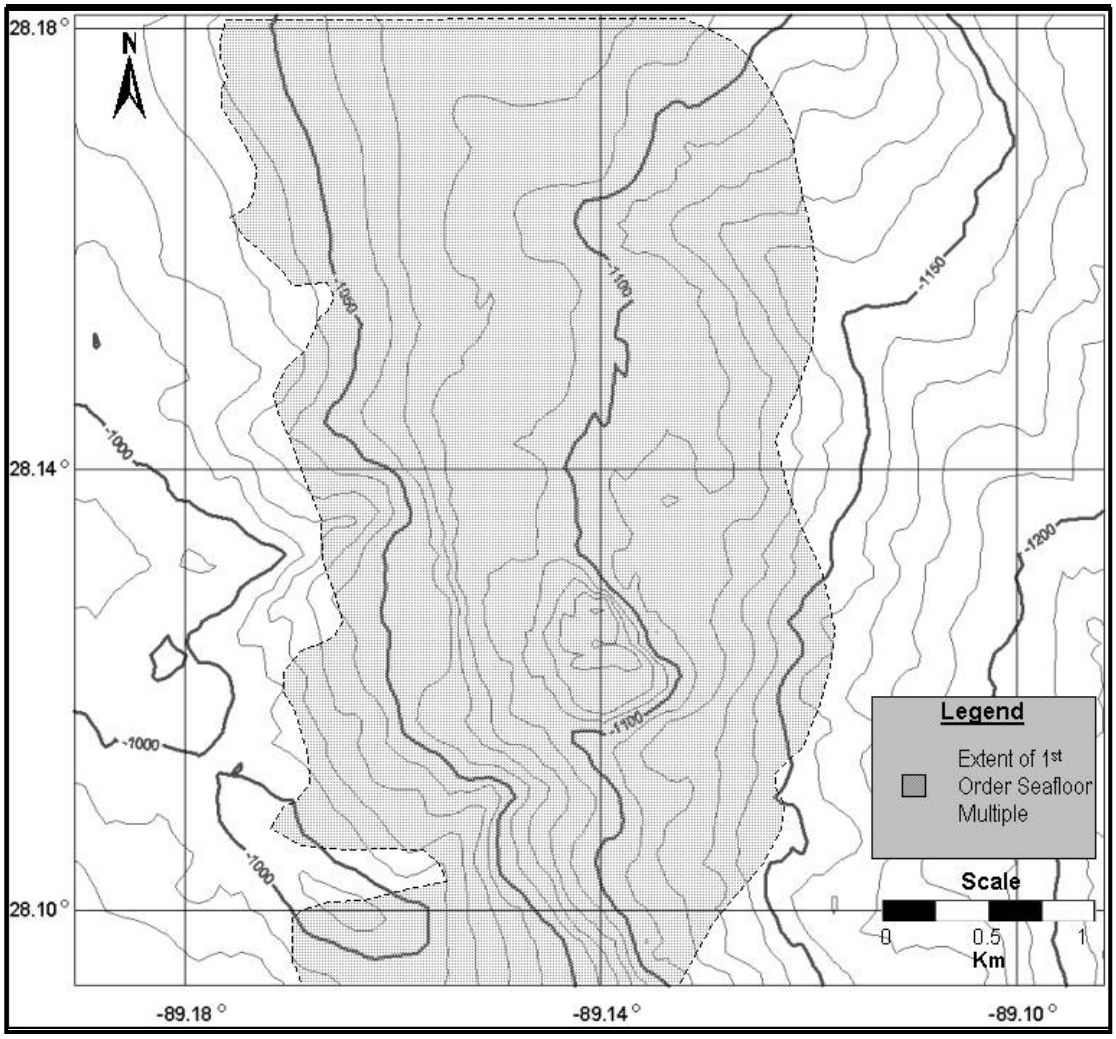

Figure 14. Bathymetric map illustrating lateral extent of 1st order seafloor multiple in the original and reprocessed 3D MCS data in the Mississippi Canyon site

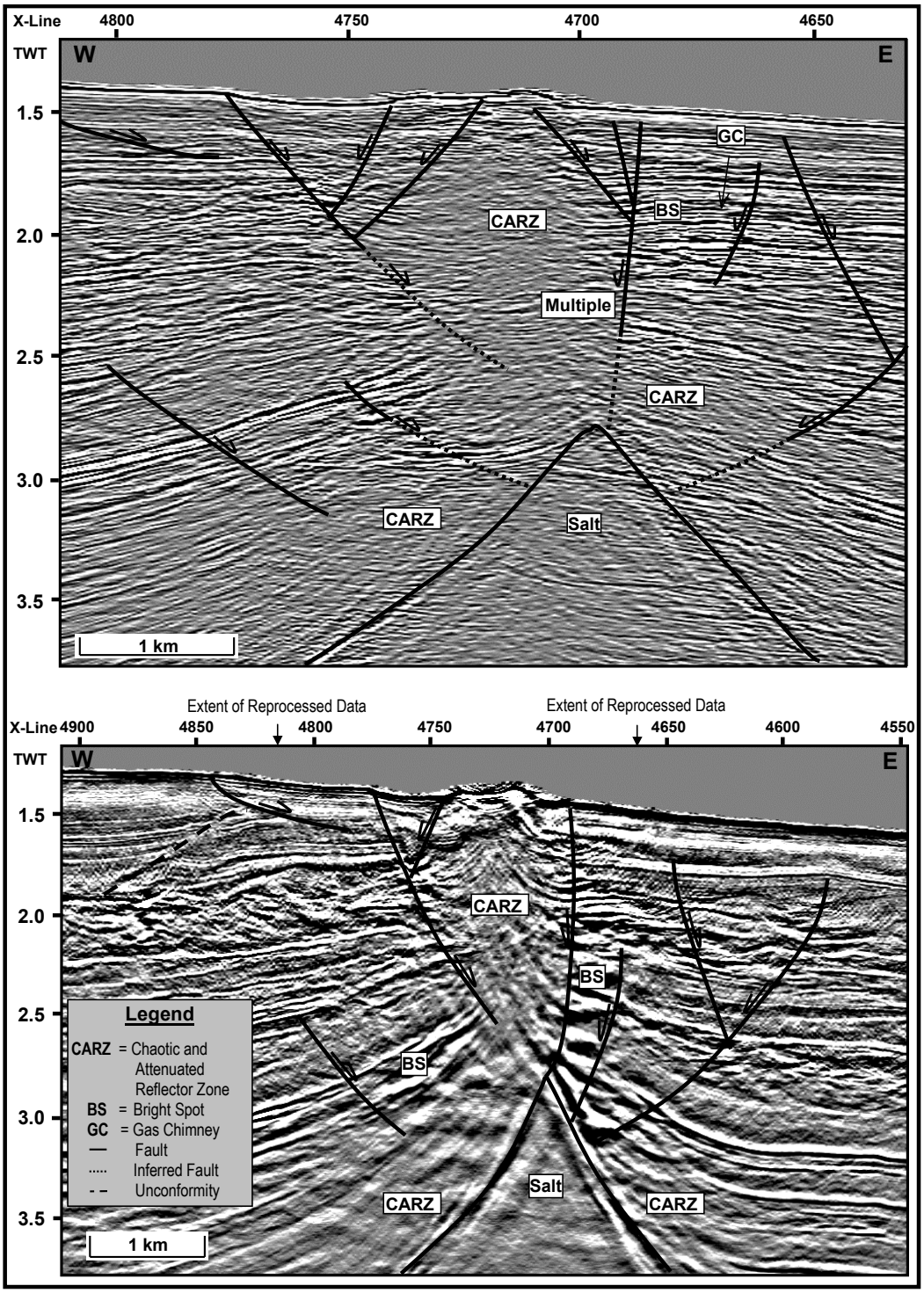

Figure 15. Cross-section of reprocessed (top) and original (bottom) 3D MCS data across west to east profile line 7660 in Mississippi Canyon site. Location in Figure 10. Conventions as in Figure 8.

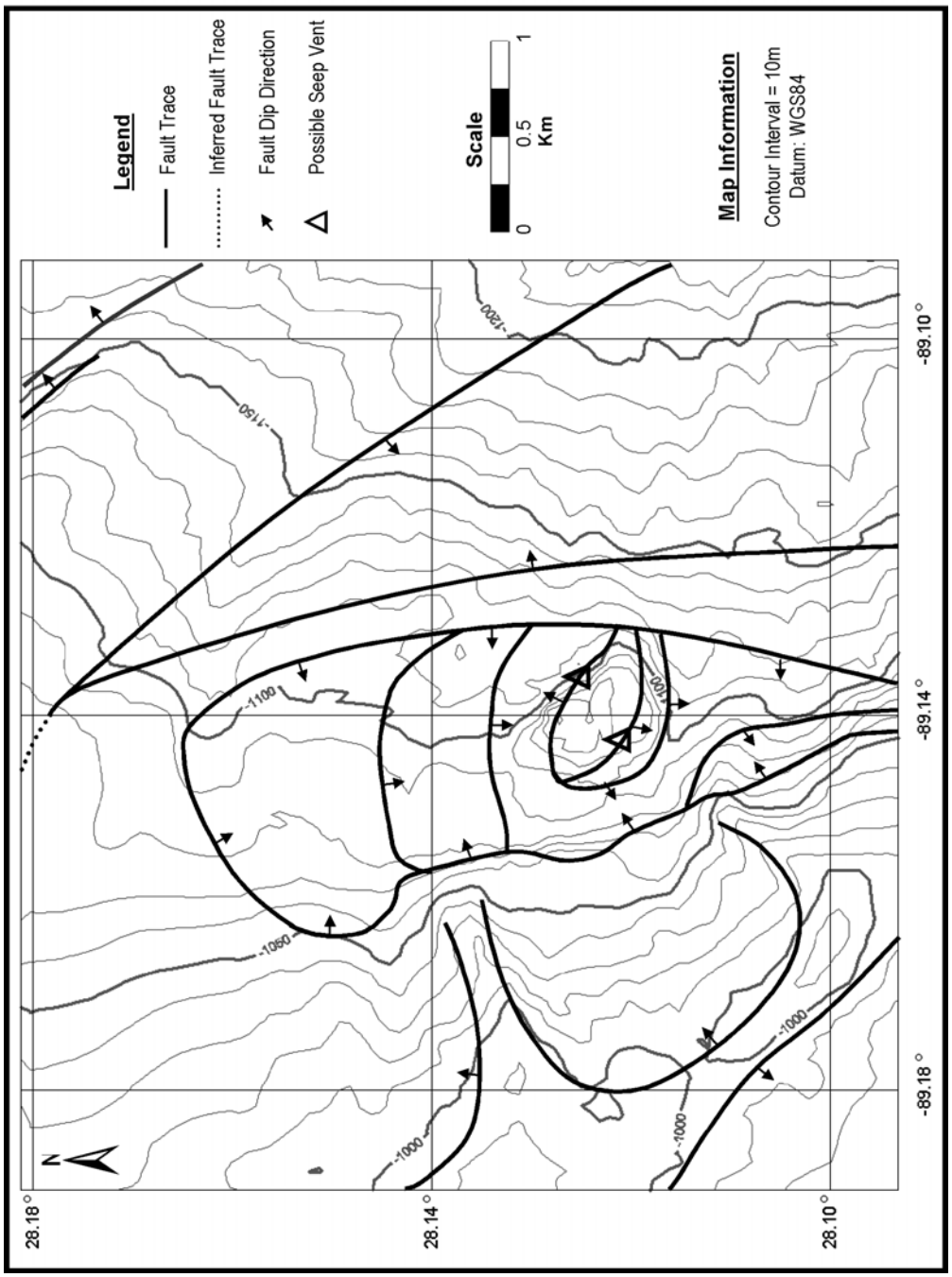

Figure 16. Map illustrating location of seep related faults as well as known and assumed vent locations in the Garden Banks area.

characterized by locally disrupted upward welling reflectors (Figure 15 top, between shot points 4650 and 4700). No other visible large scale faulting appears to occur in the survey area except in the northeast corner, where two normal faults have formed in response to the upwelling salt.

Multiple geophysical indicators of hydrocarbon fluid and gas are present in the sub-surface, most notably in the northern and central portions of the survey area. The mapping of these indicators, including zones of chaotic and attenuated reflectors, velocity pull-downs and bright spots in cross-sections and time slices shows the purported gas occupying horizons below 1.7 sec TWT in the north and pinching out about 1 to 2 kilometers south of the seep mound. Approaching the central salt ridge crest the gas appears to migrate up the northern, western and eastern faces to a prominent reflector around 1.6 sec TWT a zone of chaotic and attenuated reflectors 1 km wide to 1.5 km long. From here the hydrocarbon fluid and gas may follow pre-existing faults to expression at the seafloor.

CHAPTER IV

DISCUSSION

The focus of this study was to characterize seep activity and develop an understanding of the processes that led to seep formation in the Garden Banks and Mississippi Canyon study areas using geophysical remote sensing methods. While side-scan sonar and 3D MCS may have provided high density coverage and a detailed view of features within the sites, weaknesses are apparent in the geophysical data including: (1) the issue of resolution verses penetration with the acoustic acquisition frequency, (2) varying geophysical signature depending on acoustic frequency, and (3) lack of ground-truth verification.

With all geophysical acquisition systems there is generally a trade-off between the resolution and depth penetration of acoustic waves, depending on the frequency range used during acquisition. With an acoustic frequency of 12 kHz, the side-scan sonar data were able to provide detailed decimeter scale resolution of surficial features in the Garden Banks site, but with penetration on the order of centimeters to meters (Liu, 1997) the image is restricted to characteristics of the seafloor. On the other hand, 3D MCS with acoustic acquisition frequencies an order of magnitude less than the side-scan sonar (6-128 Hz) were able to image kilometers into the sub-surface. However, seismic array geometry and large source to receiver distances resulted in horizontal resolutions on the order of tens of meters and this resolution may prevent us from distinguishing surficial features such as small active vents and areas of narrow or isolated hard ground.

In hopes of increasing resolution capabilities, reprocessed 3D MCS data sets of the survey areas were utilized. With an increased sampling rate, fewer stacked traces and higher frequencies (20 to 128 Hz) the reprocessed data were able to identify small sub-surface features, including salt-induced faults related to seep development and fluid/gas expulsion features, which were otherwise not apparent in the original exploration data. The reprocessed data were not able to clearly and consistently image deep sub-surface reflectors such as the salt-sediment interface and horizons below the first order seafloor multiple. This makes it necessary to use both data sets for interpretation. Comparisons of seafloor amplitude data indicate that the reprocessed data were able to distinguish or enhance relatively thin or narrow features such as hard grounds, sediment flows and narrow gas bodies at a higher resolution than the original exploration data. It is worth noting that the algorithm that determines amplitude depends on where the seafloor is picked relative to the seismic wavelet. Therefore, it is possible that in areas of irregular seafloor or steep slopes, the algorithm may pick the incorrect segment of the wavelet possibly returning a false amplitude value. This could result in a false amplitude anomaly in a data set that might otherwise be attributed to the resolution capabilities of the data. For example, if a thin layer of gas were present at the seafloor, the reprocessed data, with high vertical resolution capabilities, may incorporate the gas into its seafloor response whereas the exploration data, with lower resolutions might not. The same situation could develop if a thin layer of hard ground were present at the seafloor. The reprocessed data, with a smaller detection threshold may incorporate the hard ground into the seafloor amplitude response, displaying a positive amplitude

anomaly, whereas the original data might not, such as may be occurring on the southwestern flank of the SMV in the Garden Banks area. This suggests that the high resolution data may provide a more realistic image amplitude map of the seafloor while the exploration data may provide a clearer picture of what is occurring in the near surface.

A further consequence of differing acoustic frequencies is the variation in geophysical signatures of hydrocarbon fluid and gas deposits in the geophysical record. In the Garden Banks area, areas of sub-surface reflectors are visible in the reprocessed data but appear as zones of chaotic and attenuated reflectors in the original 3D MCS data. Conversely, chaotic and attenuated reflectors in the Mississippi Canyon reprocessed MCS data appear quite clearly in the original as do bands of amplitude enhancement (bright spots). This phenomenon may be the result of the amount of gas, fluid and seep debris in the sediment column as well as the density and distribution of these deposits interacting with the frequencies of the acoustic pulse (Anderson and Bryant, 1990; Sheriff and Geldart, 1995). These differences may also be due to the properties of the sub-surface reflectors themselves (i.e., hard grounds, unconformities) affecting the down-going acoustic pulse, attenuating or reflecting the acoustic energy. It is difficult to calculate area, but the reprocessed data appears to exhibit larger areas of attenuated reflectors, possibly as a result of the higher frequencies being attenuated or scattered by sub-surface features in areas where the lower frequencies may penetrate. Previous observations of gas and fluid seepage by submersible at our seep locations (Sager et al., 1999; Sassen et al., 1999b) do not preclude us from assuming that

hydrocarbon fluid and gas is responsible for the observed geophysical indicators, but indicators can also derive from other processes including fluidized movement of sediment which can wipe out internal structure (Roberts et al., 1999). Variations are also apparent in the surficial images produced by the side-scan sonar (Garden Banks) and 3D MCS amplitude extraction. Some features can be correlated, such as sediment flows and possible active vent sites; while others, most notably fault traces and areas that may contain hard grounds might not. While this might be caused by errors in sonar cross-track positioning, it is likely the result of differences in acoustic frequencies. For instance, if a large gas or fluid deposit were disseminated below a thin surficial layer of coarse sediment or hard ground, sonar would likely register enhanced backscatter whereas the 3D MCS might display a zone of low amplitude. Differences in sonar and amplitude response suggest this may be occurring on the summit of the SMV in the Garden Banks area as well as along the fault trace at the southern edge of the survey.

Regardless of the resolution of the acquisition system, lack of direct observations or ground truth data makes definitive identification of many features difficult. Possible active vent sites, even ones returning sharply defined negative amplitude anomalies and showing evidence of recent sediment flows, such as on the NE flank of the SMV can only be tentatively identified without direct verification by submersible or ROV. Additionally, 3D MCS and sonar data can be susceptible to false targets such as those caused by errors in navigation, processing or seafloor interpretation.

Despite the inherent limitations of our geophysical data, they are nonetheless able to provide valuable insight into the geology of the seep features and the processes

that led to their formation. Many similarities exist between the seep mounds in the Garden Banks and Mississippi Canyon areas. Bathymetric and 3D MCS reflection data implies that the seep features are located atop complex fault systems within fault-induced depressions (Figures 09 (GB) and 16 (MC)). We believe that the faulting and subsequent depression formation is the result of upwelling salt as they are located directly above shallow underlying salt ridge crests. This conforms to observations from other seep investigations within the Gulf of Mexico in which the seeps were found to be oriented along fault traces and in the vicinity of shallow salt structures (Kaluza and Doyle, 1996; Reilly et al., 1996; Thrasher et al., 1996; Roberts and Carney, 1997). At the Garden Banks site, hydrocarbons (concentrated in the west and NW of the survey area) appear to be migrating along bedding planes contained by a depression in the salt to the crest of the salt ridge. Mapping of the unconformity suggests that vertical displacement on the order of hundreds of meters along the main fault may have resulted in the formation of a large linear fault system paralleling the salt ridge. The occurrence of a large vertical zone of chaotic and attenuated reflectors beneath the mud volcanoes and seafloor amplitude anomalies suggests that fluidized mud and hydrocarbons are moving along this fault system, as well as along other, possibly undetected faults masked by the gas chimney, to the seafloor creating the two mud volcanoes on the eastern flank of the depression.

The apparent formation sequence of the Mississippi Canyon seep mound is similar to that of the Garden Banks mud volcanoes. It is also situated atop a ridge in the underlying salt; whose motion likely led to the formation of complex fault systems that

surround the mound. Likewise it is located in an area characterized by geophysical indicators of hydrocarbon fluid and gas that appear to be migrating along fault systems creating a zone of chaotic and attenuated reflectors beneath the mound. In contrast, the fault system in the Mississippi Canyon area is small and graben-like as apposed to large linear regional faults. Additionally, the small size of the depression and the development of tensile faults may have allowed hydrocarbons and fluidized mud to breach the seafloor at the center of the depression creating the seep mound as opposed to the Garden Banks mud volcanoes which formed on the flank of the relative large depression. Other minor differences are also apparent, namely in the number of vent features and geographical location, but for the most part the processes of seep formation and their seepage styles appear similar between the two sites.

The 3D MCS seafloor amplitude maps proved to be useful in characterizing the seepage rates of the three large seep vent mounds in this study. In the Garden Banks area, the SMV appears to be an established high flux vent. The summit and flanks contain negative amplitude anomalies and the presence of sediment flows implies that active venting may be occurring. This is supported by the sharply defined negative amplitude responses that appear at the apparent origination points of the flows, specifically the negative responses on the northeastern and western flanks. In addition, near bottom high frequency (28 kHz) sub-bottom profiler surveys indicate that the flanks are characterized by wipeout and ringing features commonly associated with gas charged sediment (Lee, 1995; Sager et al., 1999). Submersible observations also indicate the presence of a brine pool on the southwestern summit from which a flow may have

recently occurred (Sager et al., 1999). Coring evidence indicates that abundant gas, perhaps from dissociated gas hydrate may be present in the near-surface sediments of the SMV (Sager et al., 1999). Gas hydrates tend to have an amplitude response that more closely resembles that of carbonate than free gas, making detection difficult in seismic records where both may coexist (Roberts et al., 2002). Sea bottom pressure and temperature conditions are within the hydrate stability field and massive seafloor accumulations have been found at other mud mounds (MacDonald et al., 1994). The size of the mound and the build-up of carbonate and other coarse debris on the flanks imply that the SMV, though young is likely an established high flux mud volcano.

The NMV most likely represents an established low flux seep vent. No seafloor observational data is available, but positive seafloor amplitude anomalies from its summit and flanks indicates that hard ground that may be due to carbonate or other coarse debris has built up. Additionally, the lack of sediment flow evidence and the occurrence of a fewer negative amplitude anomalies on its summit and flanks imply that the NMV is the least active of the two mud volcanoes and possibly entering the third stage of the self-sealing process hypothesized by Hovland (2002). At this stage carbonate build-up can severely limit hydrocarbon migration and venting.

In the Mississippi Canyon study area the seep mound appears to be a mature, but active seep vent owing to the build-up of bacterial mats and authigenic carbonate. Additionally, evidence of fluidized sediment flows and active hydrocarbon oil and gas venting on the summit imply that the mound is quite active. Confirmation of gas hydrates exists at this site in the form of intact samples taken during coring

operations on the summit of the seep mound (Milkov and Sassen, 2000). As in the Garden Banks area, pressure and temperature conditions are conducive for the formation and stability of gas hydrate, but no large surficial deposits were located during submersible or coring operations and MCS amplitude data is unable to differentiate between carbonate and hydrate outcrops in our data sets. Nevertheless, the size and complexity of the mound as well as the presence of multiple hard grounds, including carbonate outcrops, small gas hydrate nodules and bacterial mats implies that the mound is at a later stage of the self-sealing process. Its position at the edge of a large hydrocarbon field though, ensures that this seep mound may continue to be active indefinitely, with a succession of individual seep vents forming and sealing, only to form again elsewhere on the mound.

CHAPTER V

CONCLUSION

Several geophysical data sets were used to characterize seep features in the Garden Banks and Mississippi Canyon study areas. Side-scan sonar, where available, allowed for high resolution imaging of the seafloor and seep features, while 3D MCS provided insight into sub-surface features and structure. Additionally, MCS seafloor amplitude data was effective at characterizing the surface activity of a seep by delineating areas of negative and positive amplitudes which appear to correlate to areas of gas charged sediment and hard ground, respectively.

Differences in acoustic response give a better understanding of a two study area's structure. The 12 kHz side-scan sonar data were able to delineate individual seafloor fault traces in addition to areas of low and high backscatter associated with gas charged and disturbed sediment at decimeter scale resolution. The exploration 3D MCS data, while unable to discern small features were necessary to resolve the salt interface and features below the 1st order seafloor multiple that were otherwise poorly imaged by the reprocessed data. The reprocessed MCS data were invaluable because they were able to delineate near-surface seep related faults and fluid and gas expulsion features that where poorly shown by the low resolution exploration data.

The data implies that the SMV in the Garden Banks site is characterized as an established high flux seep vent due to signs of hard ground build up on its flanks and signs of active seepage in the form of negative amplitude anomalies on its summit and

flanks as well as the presence of fluidized mud flows appearing to emanate from its flanks. The NMV, with substantially more positive amplitude returns from its summit and flanks and fewer negative amplitude anomalies appears to be the least active and more mature of the two mud volcanoes, representing an established low flux rate seep vent. In the Mississippi Canyon the seep mound can be characterized as a mature high flux vent. The data suggest that substantial build up of hard ground has occurred on the summit and flanks of the mound with patches of negative amplitude anomalies and possible sediment flows indicating that the active seepage may be occurring. The complex relief and patchy amplitude anomalies suggest that sites of active seepage are ephemeral, either self sealing or switching to alternate locations on the mound.

The environmental conditions and processes that led to seep formation in the Garden Banks and Mississippi Canyon sites appear quite similar. The upward movement of salt to the shallow sub-surface may have led to the formation of fault-induced depressions directly above the salt crests. Geophysical indicators of hydrocarbon fluid and gas imply that hydrocarbons are migrating along bedding planes to the salt crests where they intersect the salt induced fault systems. Here they appear to continue their migration to the seafloor creating the seafloor amplitude anomalies that characterize the seeps.

REFERENCES

Anderson, A. L., and W. R. Bryant, 1987, Distribution of seafloor shallow gas in the northwestern Gulf of Mexico: Proceedings of the Offshore Technology Conference, OTC 5518, p. 295-299.

Anderson, A. L., and W. R. Bryant, 1990, Gassy sediment occurrence and properties - northern Gulf of Mexico: Geo-Marine Letters, v. 10, p. 209-220.

Behrens, E. W., 1988, Geology of a continental-slope oil seep, northern Gulf of Mexico: AAPG Bulletin, v. 72, p. 105-114.

Bryant, W. R., J. R. Bryant, M. H. Feeley, and G. R. Simmons, 1990, Physiographic and bathymetric characteristics of the continental-slope, northwest Gulf of Mexico: Geo-Marine Letters, v. 10, p. 182-199.

Corthay, J.E. II, 1998, Delineation of a massive seafloor hydrocarbon seep, over pressured aquifer sands and shallow gas reservoirs, Louisiana Continental Slope: Proceedings of the Offshore Technology Conference, OTC 8594, p. 37-56

Dimitrov, L. I., 2002, Mud Volcanoes - The most important pathway for degassing deeply buried sediments: Earth-Science Reviews, v. 59, p. 49-79.

Fish, J. P., and H. A. Carr, 1990, Sound Underwater Images: Orleans, MA, Lower Cape Publishing, 188 p.

Hovland, M., 2002, On the self-sealing nature of marine seeps: Continental Shelf Research, v. 22, p. 2387-2394.

Hovland, M., and A. G. Judd, 1988, Seabed pockmarks and seepages: Boston, Grahan and Trotman Inc., 293 p.

Kaluza, M. J., and E. H. Doyle, 1996, Detecting fluid migration in shallow sediments: continental slope environment, Gulf of Mexico, *in* D. Schumacher, and M. A. Abrams, eds., Hydrocarbon migration and its near-surface expression, AAPG Memoir 66, p. 15-26.

Kvenvolden, K. A., 1993, Gas hydrates: geological perspective and global change: Rev. Geophysics, v. 31, p. 173-187.

Lee, C. S., 1995, Geology of hydrocarbon seeps on the northern Gulf of Mexico continental slope; Ph.D dissertation, Texas A&M University, College Station, Texas, 114 p.

Limonov, A. F., T. C. E. van Weering, N. H. Kenyon, M. K. Ivanov, and L. B. Meisner, 1997, Seabed morphology and gas venting in the Black Sea mud volcano area: Observations with the MAK-1 deep-tow sidescan sonar and bottom profiler: Marine Geology, v. 137, p. 121-136.

Liu, J. Y., 1997, Surficial geological characteristics of the Alaminos Canyon, Gulf of Mexico: Ph. D. dissertation, Texas A&M University, College Station, Texas 142 p.

Lowrie, A., 2002, Sediment strength and hydrates along the northern Gulf of Mexico: Proceedings of the Offshore Technology Conference, OTC 14037, p. 7.

MacDonald, I. R., D. B. Buthman, W. W. Sager, M. B. Peccini, and N. L. J. Guinasso, 2000, Pulsed oil discharge from a mud volcano: Geology, v. 28, p. 907-910.

MacDonald, I. R., N. L. Guinasso, R. Sassen, J. M. Brooks, L. Lee, and K. T. Scott, 1994, Gas hydrate that breaches the seafloor on the continental slope of the Gulf of Mexico: Geology, v. 22, p. 699-702.

Milkov, A. V., and R. Sassen, 2000, Thickness of the gas hydrate stability zone, Gulf of Mexico continental slope: Marine and Petroleum Geology, v. 17, p. 981-991.

Mullins, A. J., 2001, Seismic interpretation of hydrocarbon seep features, Garden Banks, Gulf of Mexico: M.Sc. thesis, Texas A&M University, College Station, Texas, 97 p.

Neurauter, T. W., 1988, Mud mounds on continental slope northwestern Gulf of Mexico and their relation to hydrates and seafloor instability: Ph.D dissertation, Texas A&M University, College Station, Texas, 154 p.

Neurauter, T. W., and W. R. Bryant, 1990, Seismic expression of sedimentary volcanism on the continental-slope, northern Gulf of Mexico: Geo-Marine Letters, v. 10, p. 225-231.

Orange, D. L., J. Yun, N. Maher, J. Barry, and G. Greene, 2002, Tracking California seafloor seeps with bathymetry, backscatter and ROV's: Continental Shelf Research, v. 22, p. 2273-2290.

Reilly, J. F. I., I. R. MacDonald, E. K. Biegert, and J. M. Brooks, 1996, Geologic controls of the distribution of hydrocarbon seeps and chemosynthetic communities in the Gulf of Mexico, *in* D. Schumacher, and M. A. Abrams, eds., Hydrocarbon migration and its near-surface expression, v. AAPG Memoir 66, p. 39-62.

Riedel, M., G. D. Spence, N. R. Chapman, and R. D. Hyndman, 2002, Seismic investigations of a vent field associated with gas hydrates, offshore Vancouver Island: Journal of Geophysical Research-Oceans, v. 107 (B9), p. 1-16.

Roberts, H. H., 1992, Hydrocarbon seeps of the Louisiana continental slope: seismic amplitude signature and seafloor response: Gulf Coast Association of Geological Societies Transactions, v. XLII, p. 349-360.

Roberts, H. H., 1995, High resolution surficial geology of the Louisiana middle-to-upper continental slope: Gulf Coast Association of Geological Societies Transactions, v. XLV, p. 503-508.

Roberts, H. H., P. Aharon, R. Carney, J. Larkin, and R. Sassen, 1990, Seafloor responses to hydrocarbon seeps, Louisiana continental slope: Geo-Marine Letters, v. 10, p. 232-243.

Roberts, H. H., and R. S. Carney, 1997, Evidence of episodic fluid, gas, and sediment venting on the northern Gulf of Mexico continental slope: Economic Geology and the Bulletin of the Society of Economic Geologists, v. 92, p. 863-879.

Roberts, H. H., and E. H. Doyle, 1998, Seafloor calibration of high resolution acoustic data and amplitude rendering of the "Diapiric Hill," Garden Banks 427: Proceedings of the Offshore Technology Conference, OTC 8592, p. 19-30.

Roberts, H. H., E. H. Doyle, J. R. Booth, B. J. Clark, M. J. Kaluza, and A. Hartsook, 1996, 3D-seismic amplitude analysis of the sea floor; an important interpretive method for improved geohazards evaluations.: Proceedings of the Offshore Technology Conference, OTC 7988, p. 283-292.

Roberts, H. H., J. L. Hunt, W. W. Shedd, and R. Sassen, 2002, Surficial gas hydrates, part of the fluid and gas expulsion response spectrum: Identification from 3D seismic data: Proceedings of the Offshore Technology Conference, OTC 14033, p. 10.

Roberts, H. H., B. Kohl, D. Menzies, and G. D. Humphrey, 1999, Acoustic wipe-out zones; a paradox for interpreting seafloor geologic/ geotechnical characteristics (an example from Garden Banks 161). Proceedings of the Offshore Technology Conference, OTC 10921, p. 591-602.

Rowan, M. G., 1995, Structural styles and evolution of allochthonous salt, central Louisiana outer shelf and upper slope, in D. G. Roberts, and S. Snelson, eds., Salt tectonics, a global perspective, AAPG Memoir 65, p. 199-228.

Rowan, M. G., M. P. A. Jackson, and B. D. Trudgill, 1999, Salt-related fault families and fault welds in the northern Gulf of Mexico: AAPG Bulletin, v. 83, p. 1454-1484.

Sager, W. W., C. S. Lee, I. R. MacDonald, and W. W. Schroeder, 1999, High frequency near-bottom acoustic reflection signatures of hydrocarbon seeps on the northern Gulf of Mexico continental slope: Geo-Marine Letters, v. 18, p. 267-276.

Sager, W. W., I. R. MacDonald, W. R. Bryant, R. L. Carlson, and D. B. Prior, 1998, Digital side-scan sonar survey of Louisiana slope areas containing active oil seeps and halokinetic sediment modification: Proceedings of the Offshore Technology Conference, OTC 8595, p. 57-69.

Sager, W. W., I. R. MacDonald, and R. Hou, 2003, Geophysical signatures of mud mounds at hydrocarbon seeps on the Louisiana continental slope, northern Gulf of Mexico: Marine Geology, v. In Press.

Sassen, R., S. Joye, S. T. Sweet, D. A. DeFreitas, A. V. Milkov, and I. R. MacDonald, 1999a, Thermogenic gas hydrates and hydrocarbon gases in complex chemosynthetic communities, Gulf of Mexico continental slope: Organic Geochemistry, v. 30, p. 485-497.

Sassen, R., I. R. MacDonald, N. L. Guinasso, S. Joye, A. G. Requejo, S. T. Sweet, J. Alcala-Herrera, D. A. DeFreitas, and D. R. Schink, 1998, Bacterial methane oxidation in sea-floor gas hydrate: significance to life in extreme environments: Geology, v. 26, p. 851-854.

Sassen, R., A. V. Milkov, D. A. DeFreitas, and H. H. Roberts, 2002, Gas venting and gas hydrate stability in the northwestern Gulf of Mexico slope: Significance to sediment deformation: Proceedings of the Offshore Technology Conference, OTC 14034, p. 1-7.

Sassen, R., S. T. Sweet, A. V. Milkov, D. A. DeFreitas, G. G. Salata, and E. C. McDade, 1999b, Geology and geochemistry of gas hydrates, central Gulf of Mexico continental slope: Gulf Coast Association of Geological Societies Transactions, v. XLIX, p. 463-468.

Schuster, D. C., 1995, Deformation of allochthonous salt and evolution of related salt-structural systems, eastern Louisiana Gulf Coast, in D. G. Roberts, and S. Snelson, eds., Salt tectonics: a global perspective, AAPG Memoir 65, p. 177-198.

Sheriff, R. E., and L. P. Geldart, 1995, Exploration Seismology: New York City, Press Syndicate of the University of Cambridge, 592 p.

Thrasher, J., A. J. Fleet, S. J. Hay, M. Hovland, and S. Dueppenbecker, 1996, Understanding geology as the key to using seepage in exploration; the spectrum of seepage styles., *in* D. Schumacher, and M. A. Abrams, eds., Hydrocarbon migration and its near-surface expression., AAPG Memoir 66, p. 223-241.

Trabant, T. K., 1996, Use of 3D-exploration seismic data for geohazard analysis: Proceedings of the Offshore Technology Conference, OTC 7991, p. 319-326.

VITA

Ryan Douglas Thomas was born in North Carolina, but has spent the majority of his life in Ohio and Michigan. He attended Michigan State University where in June of 1999 he fulfilled the requirements for a B.S. in Geological Sciences and a B.A. in German. Ryan has attended Texas A&M University where he completed a Master of Science in oceanography specializing in marine geology and geophysics. After completion he will be moving to Olympia, Washington to pursue a career in marine geophysical consulting and spend some time enjoying the outdoors. He can be reached at 42583 Whitman Way, Novi, MI 48377.